

# A MYB/bHLH complex regulates tissue-specific anthocyanin biosynthesis in the inner pericarp of red-centered kiwifruit *Actinidia chinensis* cv. Hongyang

Lihuan Wang<sup>1,2,†</sup>, Wei Tang<sup>2,3,†,\*</sup>, Yawen Hu<sup>1</sup>, Yabin Zhang<sup>1</sup>, Jiaqi Sun<sup>1</sup>, Xiuhong Guo<sup>1</sup>, Han Lu<sup>3</sup>, Ying Yang<sup>2</sup>, Congbing Fang<sup>2</sup>, Xiangli Niu<sup>2,3</sup>, Junyang Yue<sup>2,3</sup>, Zhangjun Fei<sup>4,5</sup> and Yongsheng Liu<sup>1,2,3,\*</sup>

<sup>1</sup>Ministry of Education Key Laboratory for Bio-resource and Eco-environment, College of Life Science, State Key Laboratory of Hydraulics and Mountain River Engineering, Sichuan University, Chengdu 610064, China,

<sup>2</sup>School of Horticulture and State Key Laboratory of Tea Plant Biology and Utilization, Anhui Agricultural University, Hefei 230036, China,

<sup>3</sup>School of Biotechnology and Food Engineering, Hefei University of Technology, Hefei 230009, China,

<sup>4</sup>Boyce Thompson Institute, Cornell University, Ithaca, NY, 14853, USA, and

<sup>5</sup>USDA-Agricultural Research Service, Robert W. Holley Center for Agriculture and Health, Ithaca, NY, 14853, USA

Received 25 July 2018; revised 13 March 2019; accepted 19 March 2019; published online 26 March 2019.

\*For correspondence (e-mails liuyongsheng1122@hfut.edu.cn; tangweitw@aliyun.com).

†These authors contributed equally to this work.

## SUMMARY

Many *Actinidia* cultivars are characterized by anthocyanin accumulation, specifically in the inner pericarp, but the underlying regulatory mechanism remains elusive. Here we report two interacting transcription factors, AcMYB123 and AcbHLH42, that regulate tissue-specific anthocyanin biosynthesis in the inner pericarp of *Actinidia chinensis* cv. Hongyang. Through transcriptome profiling analysis we identified five MYB and three bHLH transcription factors that were upregulated in the inner pericarp. We show that the combinatorial action of two of them, AcMYB123 and AcbHLH42, is required for activating promoters of *AcANS* and *AcF3GT1* that encode the dedicated enzymes for anthocyanin biosynthesis. The presence of anthocyanin in the inner pericarp appears to be tightly associated with elevated expression of *AcMYB123* and *AcbHLH42*. RNA interference repression of *AcMYB123*, *AcbHLH42*, *AcF3GT1* and *AcANS* in 'Hongyang' fruits resulted in significantly reduced anthocyanin biosynthesis. Using both transient assays in *Nicotiana tabacum* leaves or *Actinidia arguta* fruits and stable transformation in *Arabidopsis*, we demonstrate that co-expression of *AcMYB123* and *AcbHLH42* is a prerequisite for anthocyanin production by activating transcription of *AcF3GT1* and *AcANS* or the homologous genes. Phylogenetic analysis suggests that AcMYB123 or AcbHLH42 are closely related to TT2 or TT8, respectively, which determines proanthocyanidin biosynthesis in *Arabidopsis*, and to anthocyanin regulators in monocots rather than regulators in dicots. All these experimental results suggest that AcMYB123 and AcbHLH42 are the components involved in spatiotemporal regulation of anthocyanin biosynthesis specifically in the inner pericarp of kiwifruit.

**Keywords:** anthocyanin, *Actinidian*, MYB, bHLH, transcription factor.

## INTRODUCTION

Anthocyanins are flavonoids that range in color from red to blue and play multiple roles in the responses of plant to environmental stresses, herbivores and pathogens, the attraction of pollinators, and seed dispersal, and have a profound impact on food quality beneficial to human health (Winkel-Shirley, 2001; Xie *et al.*, 2012; Xu *et al.*, 2015). Anthocyanins and other flavonoids are synthesized primarily through regulation of genes coding for enzymes in the phenylpropanoid metabolic pathway (Hichri *et al.*,

2011). These structural genes are well characterized in a range of plant species (Boss *et al.*, 1996; Honda *et al.*, 2002; Grotewold, 2006; Huguene *et al.*, 2009). The early biosynthetic steps are catalyzed by chalcone synthase (CHS), chalcone isomerase (CHI), flavanone 3-hydroxylase (F3H) and flavonoid 3'-hydroxylase (F3'H), resulting in the production of common precursors (i.e. dihydroflavonols), while the late steps of the pathway include downstream enzymes of dihydroflavonol 4-reductase (DFR), leucoanthocyanidin dioxygenase/anthocyanidin synthase (LDOX/

ANS), 3-glycosyltransferase (3-GT) and leucoanthocyanidin reductase (LAR) or anthocyanidin reductase (ANR)/BANYULS that give rise to anthocyanin/proanthocyanidin production (Xie *et al.*, 2003; Ben-Simhon *et al.*, 2011; Liu *et al.*, 2013; Schaart *et al.*, 2013; Shen *et al.*, 2014).

There is accumulating evidence to support the suggestion that expression of the flavonoid biosynthetic genes is tightly controlled by the well-conserved MYB-bHLH-WD40 (MBW) complex in higher plants (Baudry *et al.*, 2004; Feller *et al.*, 2011; Patra *et al.*, 2013; Xu *et al.*, 2015). This complex is composed of MYB and basic helix-loop-helix (bHLH) transcription factors (TFs), together with WD40 repeat proteins that spatiotemporally regulate flavonoid production by binding to the promoters of structural genes to activate their expression. Plant MYBs have evolved into a large gene family with diverse functions (Tako *et al.*, 2006). The R2R3 MYB subfamily is the largest group present in higher plants; it possesses a highly conserved DNA-binding domain containing up to two imperfect repeats, R2 and R3 (Jin and Martin, 1999). The R2R3-MYBs play pivotal roles in flavonoid accumulation in many plants. In *Arabidopsis*, three closely related R2R3-MYB proteins, MYB11, MYB12 and MYB111, participate in transcriptional activation of the early biosynthetic genes *CHS*, *CHI* and *F3H* (Mehrtens, 2005; Stracke *et al.*, 2007), whereas R2R3-MYB TFs PAP1, PAP2, MYB113, MYB114 and TT2 activate the late biosynthesis enzymes (Borevitz *et al.*, 2000; Tohge *et al.*, 2005; Lea *et al.*, 2007; Gonzalez *et al.*, 2008; Lillo *et al.*, 2008; Li *et al.*, 2014; Xu *et al.*, 2015). Intriguingly, the R3-MYB protein MYBL2 or the R2R3-MYB protein MYB27 containing a C-terminal EAR motif acts as an inhibitor of flavonoid biosynthesis (Dubos *et al.*, 2008; Matsui *et al.*, 2008; Albert *et al.*, 2014). A number of R2R3-MYB homologs involved in the regulation of tissue-specific flavonoid accumulation have been identified in various crops (Walker *et al.*, 2007; Deluc *et al.*, 2008; Feng *et al.*, 2010; Xie *et al.*, 2012; Schaart *et al.*, 2013; Yao *et al.*, 2017).

The R3 repeat in R2R3 MYB proteins confers protein-protein interaction ability, especially with the bHLH TFs (Grotewold *et al.*, 2000). It has been shown that the binding affinity of MYB to the *cis*-element of the target gene is partially regulated by the bHLH partners (Hichri *et al.*, 2011). In *Arabidopsis*, several bHLH TFs, such as GL3, EGL3 and TT8, have been shown to interact with R2R3-MYB proteins and function in the regulation of flavonoid biosynthesis (Nesi *et al.*, 2000; Gonzalez *et al.*, 2008; Xu *et al.*, 2015). Numerous bHLHs that participate in flavonoid metabolic regulation have been identified in other plants (Chandler, 1989; Ludwig *et al.*, 1989; Hichri *et al.*, 2010; Matus *et al.*, 2010; Xie *et al.*, 2012; Schaart *et al.*, 2013; Uematsu *et al.*, 2014; Yao *et al.*, 2017). Of these, many have been shown to regulate a variety of cellular events including different branches of flavonoid biosynthesis, vacuole acidification and epidermal cell fate (Hichri *et al.*,

2011; Xu *et al.*, 2015). As an essential component in the MBW complex that affects flavonoid biosynthesis, several WD40-repeat proteins, such as TTG1, have been characterized in different plants (Walker *et al.*, 1999; Carey *et al.*, 2004; An *et al.*, 2012; Schaart *et al.*, 2013).

In genus *Actinidia* (kiwifruit), accumulation of anthocyanins, the major pigmented group of flavonoid compounds, may occur in all fruit tissues or may be restricted to the fruit skin as a blush, to the fruit pericarp or to only part of the pericarp, usually the inner pericarp (Montefiori *et al.*, 2009). Genes associated with anthocyanin metabolism in kiwifruit have been studied. The key anthocyanin biosynthetic glycosyltransferases (AcF3GT1 and AcF3GGT1) have been characterized in red-fleshed *Actinidia chinensis* cv. Hort22D and the expression of *AcF3GT1* in fruit inner pericarp is required for anthocyanin biosynthesis (Montefiori *et al.*, 2011). The first R2R3 MYB TF (*MYB110a*) determining anthocyanin accumulation in kiwifruit petal was isolated using *Actinidia* hybrid families segregating for red and white petal color (Fraser *et al.*, 2013). *AcMYB110* was also shown as an important R2R3-MYB gene in regulating anthocyanin accumulation in the fruit of red-fleshed *A. chinensis* cv. Hongyang, probably by activating the transcription of *DFR*, *ANS* and *F3GT1* (Liu *et al.*, 2017). Upregulation of MYB members (*MYBA1-1* and *MYB5-1*) by low temperature could effectively enhance anthocyanin accumulation in kiwifruit during storage through transcriptional activation of *ANS1*, *ANS2*, *DFR1*, *DFR2* and *UFGT2* (Li *et al.*, 2017a). In 'Hongyang', the expression of *AcMYB75* was closely related to anthocyanin accumulation during fruit development and its coding protein was shown specifically to bind the promoter of the anthocyanin biosynthesis gene *ANS* in a yeast one-hybrid system and *in vivo*. The overexpression of *AcMYB75* in *Arabidopsis* plants significantly accelerated biosynthetic gene expression and anthocyanin accumulation (Li *et al.*, 2017b). By contrast, high temperature has been reported to suppress the expression of *AcMYB1* that contributes to reduced anthocyanin accumulation in kiwifruit (Man *et al.*, 2015). Transregulation assays using promoters of anthocyanin pathway genes demonstrate that activation of the promoters by MYB regulators strictly relies on a bHLH partner (Hichri *et al.*, 2010). However, a bHLH protein has still to be functionally characterized in kiwifruit.

In order to gain more insight into the regulatory network of anthocyanin biosynthesis in the inner pericarp of red-centered kiwifruit cultivars, a functional genomics approach was employed, with the aim of identifying regulators controlling tissue-specific accumulation of anthocyanin. We constructed and sequenced RNA sequencing (RNA-Seq) libraries derived from inner and outer pericarp of *A. chinensis* cv. Hongyang. Based on the RNA-Seq analysis, we identified differentially expressed genes putatively involved in anthocyanin metabolism; these included eight

putative TFs (five MYBs and three bHLHs) and two late biosynthetic genes homologous to *ANS* (anthocyanidin synthase) and *F3GT1* (flavonoid 3-*O*-glucosyltransferase). Subsequent molecular and biochemical characterizations demonstrated that simultaneous expression of *AcMYB123* (NCBI accession no. MH643775) and *AcbHLH42* (NCBI accession no. MH643776) and their combinatorial action are able to elevate anthocyanin biosynthesis by activating the expression of genes in the anthocyanin biosynthetic pathway. We also provide evidence showing that it is the unique interaction between *AcMYB123* and *AcbHLH42* that dramatically modulates the expression of two flavonoid late structural genes, namely *AcANS* and *AcF3GT1*, supporting a major regulatory role for *AcMYB123/AcbHLH42* in tissue-specific anthocyanin metabolism in kiwifruit.

## RESULTS

### Differentially expressed genes between inner and outer pericarp revealed by RNA-Seq

To identify differentially expressed genes (DEGs) that might play roles in anthocyanin biosynthesis, four RNA-Seq libraries, two from the inner and two from the outer pericarp of kiwifruits collected at 90 days after anthesis (DAA), were constructed and sequenced (NCBI accession no. GSE108099). The transcriptome profiling data showed high reproducibility between the biological replicates (Figure S1 in the online Supporting Information). After removing adaptor sequences and low-quality reads, a total of 18 203 332, 9 356 430, 11 006 231 and 11 314 375 high-quality cleaned reads, respectively, were obtained from these four libraries. Among them, approximately 93% could be aligned to the kiwifruit genome (Huang *et al.*, 2013; Yue *et al.*, 2015). In total, we identified 450 genes that were significantly upregulated and 416 genes that were significantly downregulated in the inner pericarp compared with the outer pericarp (Table S1).

We then checked DEGs from the MYB, bHLH and WD40 families, which are known to be potential regulators of anthocyanin biosynthesis, as well as structural genes in the anthocyanin biosynthetic pathway. A total of ten candidate genes significantly upregulated in the inner pericarp were identified, including five MYB homologs *AcMYB44* (Acc23779/Ach21g298761), *AcMYB3R-1* (Acc19986/Ach00g6380251), *AcMYB3R-5* (Acc16851/Ach15g109311), *AcMYBPA1* (Acc08348/Ach08g104391) and *AcMYB123* (Acc28234/Ach24g242211), three bHLH homologs *AcbHLH42* (Acc19563/Ach17g348381.2), *AcGL3* (Acc20018/Ach18g244201) and *AcEGL3* (Acc20202/Ach18g071731) and two structural genes, an anthocyanidin synthase, *AcANS* (Acc28876/Ach00g361621), and a flavonoid 3-*O*-glucosyltransferase, *AcF3GT1* (Acc20131/Ach18g209671) (Huang *et al.*, 2013; Pilkington *et al.*, 2018). Interestingly, no differentially expressed WD40 genes were identified as MBW

component candidates putatively contributing to the different anthocyanin levels between the inner and outer fruit pericarp of Hongyang. The upregulation of the above ten genes in the inner pericarp at 90 DAA was confirmed by a quantitative (q)RT-PCR analysis (Figure S2).

*AcMYBPA1* and *AcMYB123* are typical R2R3 MYB proteins with a characteristic N-terminal R2R3 domain containing a conserved motif (D/E)LX<sub>2</sub>(R-K)X<sub>3</sub>LX<sub>6</sub>LX<sub>3</sub>R putatively interacting with a bHLH partner (Figure S3a), and *AcMYB123* is most closely related to the Arabidopsis TT2/AtMYB123 protein (Figure S3b). *AcMYB44*, *AcMYB3R-1* and *AcMYB3R-5* lack the highly conserved motif at the R2R3 domain. To our surprise, the protein sequences from the characterized anthocyanin-related MYBs, including *AcMYB10* (Fraser *et al.*, 2013), *AcMYB1* (Man *et al.*, 2015), *AcMYBF110* (Liu *et al.*, 2017) and *AcMYB75* (Li *et al.*, 2017b), are almost identical (Figures S3b and S4) and mapped to the same annotated gene (Acc00493) of the 'Red5' genome (Pilkington *et al.*, 2018). Similar analysis showed that all of *AcbHLH42*, *AcGL3* and *AcEGL3* are R/B-like bHLH proteins from the subgroup IIIf possessing N-terminal MYB interaction region (MIR) with three conserved motifs designated as 11, 18 and 13 box and a C-terminal basic-helix1-loop-helix2 (bHLH) domain (Figure S5a) and *AcbHLH42* is most closely related to Arabidopsis TT8/AtbHLH042 protein (Figure S5b).

### Transcriptional activation of *AcF3GT1* or *AcANS* by co-expression of *AcMYBs* and *AcbHLHs*

*AcF3GT1* encodes a flavonoid 3-*O*-glucosyltransferase, a committed enzyme required for anthocyanin production in kiwifruit, and its expression could be activated by the MYB-bHLH-WD40 complex (Montefiori *et al.*, 2011). Therefore, we postulated that the tissue-specific elevation of *AcF3GT1* expression at the inner pericarp could result from the combined upregulation of one of the *AcMYB/AcbHLH* pairs revealed by our transcriptome profiling data. To test this hypothesis, the promoter of *AcF3GT1* was isolated and used to drive GUS (*uidA* gene) reporter expression by constructing *pAcF3GT1::GUS*. Meanwhile, coding regions derived from the five *AcMYB* and the three *AcbHLH* genes in 'Hongyang' were also isolated and constructed into the plant expression vector pHB under the 2× CaMV 35S promoter. We employed *Agrobacterium*-mediated transient expression assays to test the transcriptional activation of *AcF3GT1* by either one of the eight TFs (five *AcMYBs* and three *AcbHLHs*) alone, or one of the 15 individual *AcMYB/AcbHLH* combinations (five *AcMYBs* × three *AcbHLHs*). Construct *pAcF3GT1::GUS* alone, or combined with one of the 35S::*AcMYBs* or 35S::*AcbHLHs*, or combined with one of the 35S::*AcMYB/35S::AcbHLH* pairs, was syringe-infiltrated into the abaxial surfaces of expanding *Nicotiana benthamiana* leaves. The empty vector (35S::GUS) served as a positive control. Using a histochemical staining

assay, no GUS signal was detected in the *pAcF3GT1::GUS*-infiltrated leaves, in sharp contrast to the strong GUS signal visualized in the *35S::GUS*-infiltrated leaves (Figure 1a). Meanwhile, no GUS signal was visible in any of the leaf samples infiltrated by different combinations of *pAcF3GT1::GUS* with individual *35S::AcMYBs*, *35S::AcbHLHs* or *35S::AcMYB/35S::AcbHLH* pairs, with the exception that a strong GUS signal was observed in the leaf samples co-expressing *pAcF3GT1::GUS*, *35S::AcMYB123* and *35S::AcbHLH42* (Figure 1a). To more precisely measure the GUS expression level, we performed a quantitative GUS assay. Leaf samples expressing *pAcF3GT1::GUS* or *35S::GUS* alone, or co-expressing *pAcF3GT1::GUS/35S::AcMYB123* or *pAcF3GT1::GUS/35S::AcbHLH42* or *pAcF3GT1::GUS/35S::AcMYB123/AcbHLH42*, were harvested. Consistently, only the *pAcF3GT1::GUS/35S::AcMYB123/35S::AcbHLH42*-infiltrated leaf samples, similar to the control vector *35S::GUS*, possessed the capacity to catalyze the substrate 4-methylumbelliferyl  $\beta$ -D-glucuronide (4-MUG) to form a large amount of 4-methylumbelliferone (4-MU) (Figure 1b). In addition, the promoter of *AcANS* (another upregulated structural gene in the inner pericarp) was isolated and used to drive GUS reporter expression by constructing *pAcANS::GUS*. Similar to that of *35S::GUS*, strong GUS signal was self-activated upon the infiltration of *Agrobacterium tumefaciens* strain GV3101 harboring the *pAcANS::GUS* vector (Figure 1a), and the reporter product was significantly increased when co-expressed with both *35S::AcMYB123* and *35S::AcbHLH42* (Figure 1c). These results suggest that simultaneous expression of both *AcMYB123* and *AcbHLH42* can activate the function of the promoters of *AcF3GT1* and *AcANS*.

### Interaction between *AcMYB123* and *AcbHLH42*

To demonstrate the interaction of *AcMYB123* and *AcbHLH42*, bimolecular fluorescence complementation (BiFC) assays were performed. Two fusion protein vectors, pSPYNE-*AcMYB123* and pSPYCE-*AcbHLH42*, were constructed and co-transformed into *N. benthamiana* leaf protoplast cells. As a result, a strong yellow fluorescent signal was observed in the nucleus transformed with both pSPYNE-*AcMYB123* and pSPYCE-*AcbHLH42*. No fluorescent signal was detected in cells co-transformed with pSPYNE-*AcMYB123* and empty vector pSPYCE, or with pSPYCE-*AcbHLH42* and empty vector pSPYNE, or with the

two empty vectors (Figure 2a). In addition, to verify the subcellular localization of *AcMYB123* and *AcbHLH42* in plant cells, green fluorescent protein (GFP) was fused in-frame to their C-terminals. Transiently expressed *AcMYB123-GFP* or *AcbHLH42-GFP* protein signal was detected exclusively in the nucleus, whereas the positive control showed GFP signal throughout the cytoplasm and nucleus and an untransformed plant protoplast as a negative control showed no fluorescence signal (Figure S6). These analyses indicate that both *AcMYB123* and *AcbHLH42* are nuclear proteins and are able to interact physically.

To further demonstrate whether *AcMYB123* could form a complex with *AcbHLH42*, co-immunoprecipitation (Co-IP) assays were conducted using the tobacco transient expression system. To this end, we co-expressed tagged fusion proteins *AcMYB123-HA* and *AcbHLH42-FLAG* in tobacco leaves. Total proteins from the infiltrated leaves were used to perform immunoprecipitation with an  $\alpha$ -hemagglutinin (HA) affinity matrix. As a result, *AcMYB123-HA* was effectively co-immunoprecipitated with *AcbHLH42-FLAG*. *AcbHLH42-FLAG* could be detected in the *AcMYB123-HA* immunocomplex captured by the  $\alpha$ -HA antibody (Figure 2b). Similarly, *AcMYB123-HA* could also be co-immunoprecipitated with *AcbHLH42-FLAG* by the  $\alpha$ -FLAG antibody (Figure 2b). These analyses further suggest that *AcMYB123* is physically associated with *AcbHLH42*.

In addition, similar experiments were conducted to test the possibility of interaction between *AcMYB123/AcbHLH42* and the previously identified anthocyanin regulator *AcMYBF110* (Liu *et al.*, 2017). The BiFC and Co-IP assays showed that, in contrast to no interaction signal being detected between *AcMYB123* and *AcMYBF110* (Figure S7a,b), bona fide physical interaction existed between *AcMYBF110* and *AcbHLH42* (Figure S7a,c).

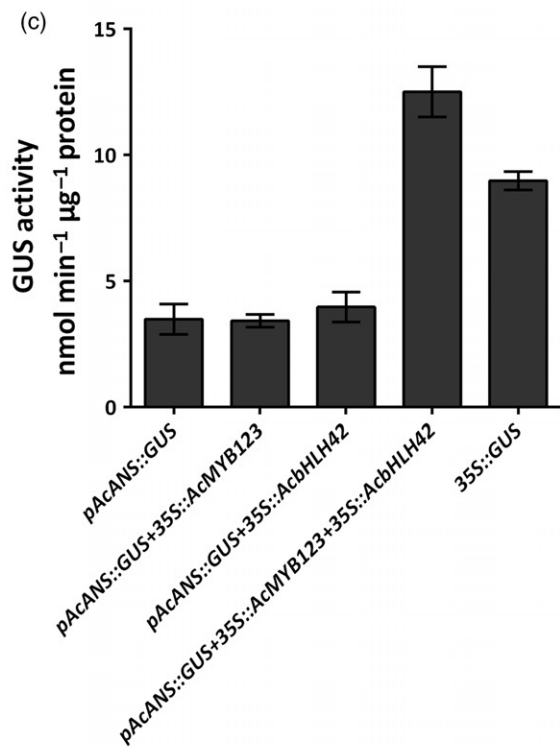
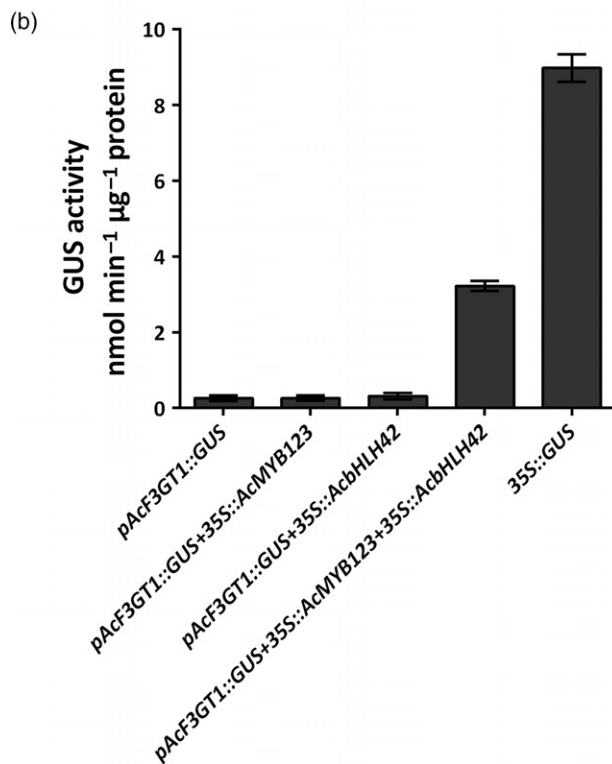
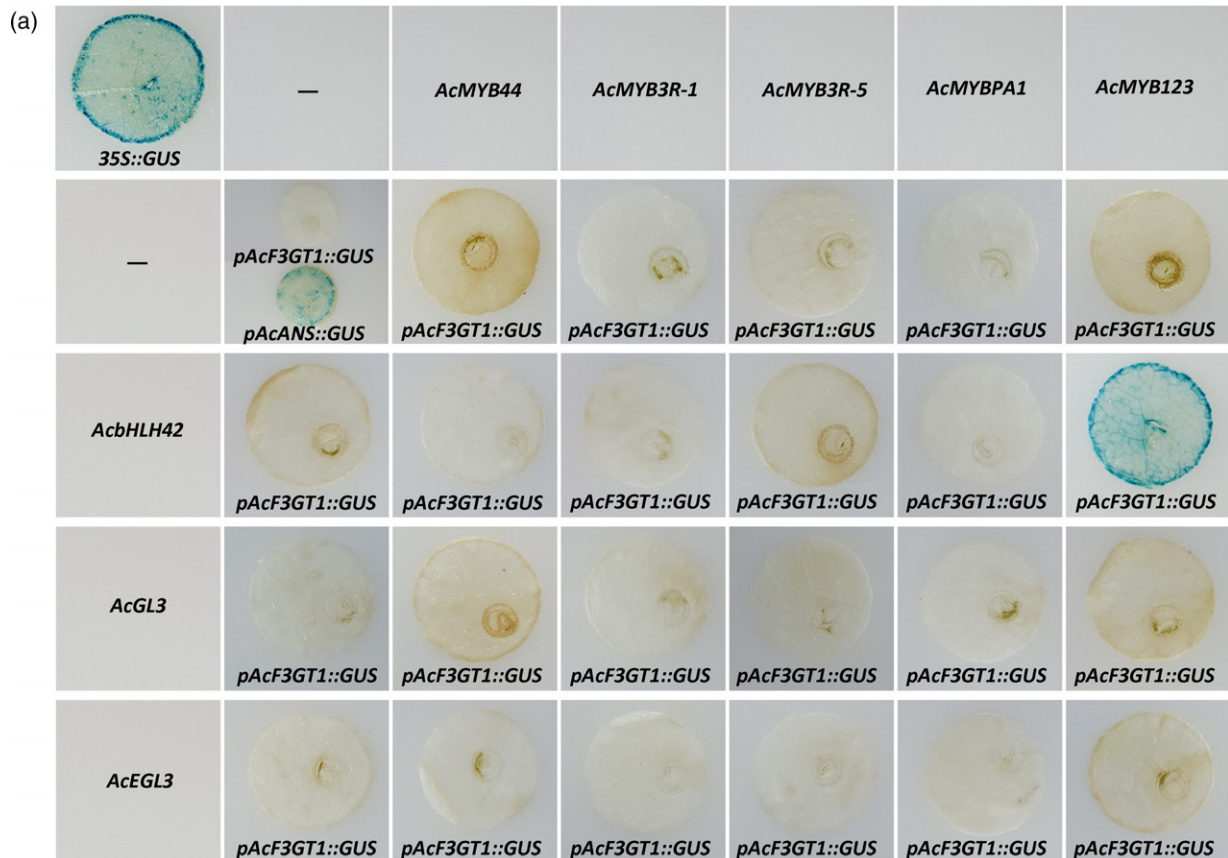
### Tissue-specific anthocyanin accumulation is associated with coordinated action of *AcMYB123*, *AcbHLH42*, *AcF3GT1* and *AcANS* during fruit development and ripening

We next examined if the difference in anthocyanin accumulation between the inner and outer pericarp of 'Hongyang' is correlated with the differential expression of *AcMYB123*, *AcbHLH42*, *AcF3GT1* and *AcANS* uncovered by our transcriptome analysis. Fruit tissues at 40, 60, 80, 90, 100 and 120 DAA were sampled (Figure 3a). Apparent

**Figure 1.** The GUS activities under control of *AcF3GT1* and *AcANS* promoters.

(a) Schematic diagram of GUS activity detected using histochemical staining in transiently expressed *Nicotiana benthamiana* leaves. *Agrobacterium tumefaciens* strain GV3101 harboring *pAcANS::GUS*, or *pAcF3GT1::GUS*, or *35S::GUS*, or *pAcF3GT1::GUS* combined with one of the *35S::AcMYB* or *35S::AcbHLH*, or one of the *35S::AcMYB/35S::AcbHLH* pairs, or *pAcANS::GUS* combined with *35S::AcMYB123/35S::AcbHLH42* was separately syringe-infiltrated into the abaxial surfaces of expanding *N. benthamiana* leaves. Construct *35S::GUS* served as a positive control. The blue color indicates activated GUS activity.

(b), (c) The GUS activity driven by *AcF3GT1* (b) or *AcANS* (c) promoter detected by fluorometric assay and expressed as nmol 4-methylumbelliferone  $\mu\text{g}^{-1}$  protein  $\text{min}^{-1}$ . Data are mean  $\pm$  SD of three independent assays of leaf extracts.



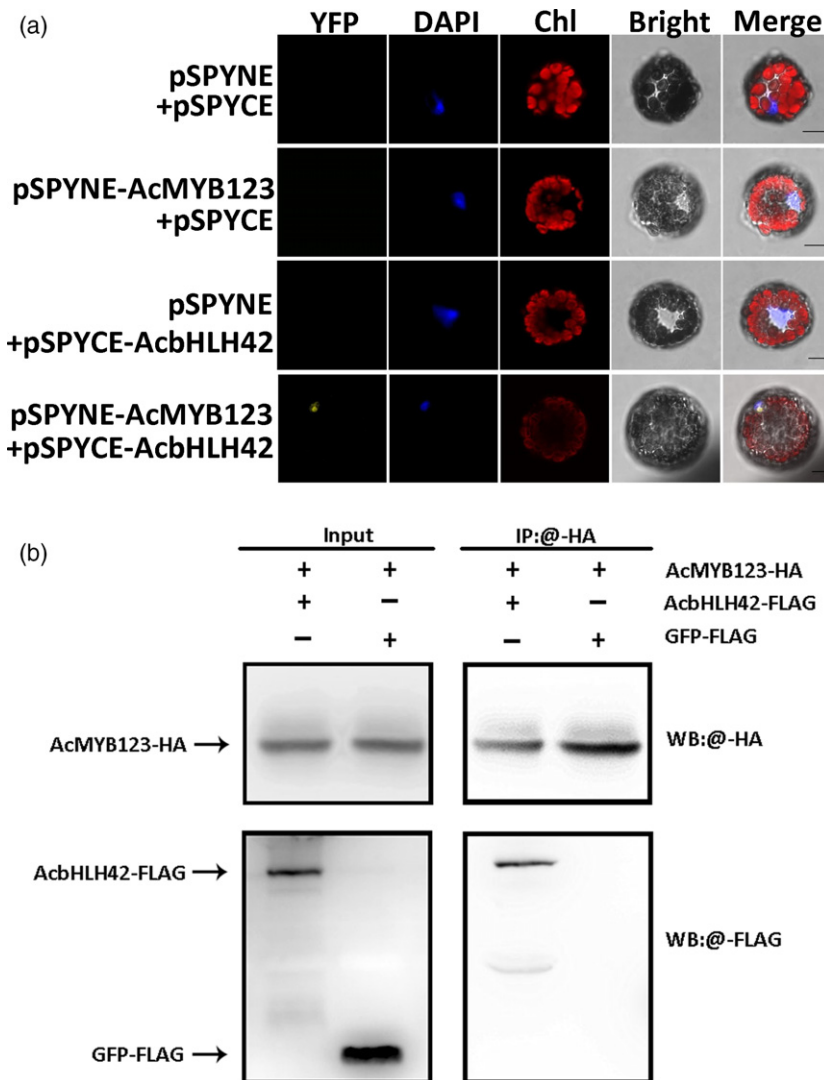


**Figure 2.** Interaction between AcMYB123 and AcbHLH42.

(a) Bimolecular fluorescence complementation (BiFC) of yellow fluorescent protein (YFP0) verifying interaction between AcMYB123 and AcbHLH42 in *Nicotiana benthamiana* protoplasts. Construct pairs were transiently co-expressed in *N. benthamiana* protoplasts. The BiFC fluorescence is shown as YFP signal determined 10 h after protoplast transformation. YFP, YFP fluorescence; DAPI, nucleus stained with 4',6-diamidino-2-phenylindole (DAPI); Chl, chlorophyll autofluorescence; Bright, a complete protoplast cell; Merge, combined fluorescence from YFP, DAPI, Chl and Bright fields. Scale bars: 10  $\mu$ m.

(b) Determination of *in vivo* interaction of AcMYB123 and AcbHLH42 by co-immunoprecipitation assays using  $\alpha$ -HA or  $\alpha$ -FLAG antibody. *Agrobacterium tumefaciens* GV3101 harboring the epitope-tagged constructs, as indicated, were syringe-infiltrated into *N. benthamiana* leaves. The GFP-FLAG construct was included as a negative control. Thirty-six hours after *Agrobacterium* infiltration, total proteins were extracted for immunoprecipitation analysis with  $\alpha$ -hemagglutinin (HA) affinity matrix, followed by Western blotting using  $\alpha$ -HA or  $\alpha$ -FLAG antibody to determine the protein-protein interaction. Arrows indicate the target protein bands.

red color emerged at 80 DAA specifically in the inner pericarp and the content of anthocyanin increased rapidly at this stage. By contrast, anthocyanin accumulation was hardly detected in the outer pericarp throughout the developmental stages (Figures 3a,b and S8). We then used qRT-PCR analysis to compare the expression patterns of *AcMYB110*, *AcMYB123*, *AcbHLH42*, *AcF3GT1* and *AcANS* between inner and outer pericarp at different developmental stages. As shown in Figure 3c–g, a large quantity of mRNA derived from *AcMYB110*, *AcMYB123*, *AcbHLH42*, *AcF3GT1* and *AcANS* was observed in the inner pericarp at 80 and 90 DAA, strikingly contrasting with the much lower and unchanged expression levels in the outer pericarp throughout fruit development. To further demonstrate the correlation between the tissue-specific anthocyanin accumulation and the increased expression of *AcMYB110*, *AcMYB123*, *AcbHLH42*, *AcF3GT1* and *AcANS*, additional *Actinidia* cultivars were

investigated, including red-fleshed *A. chinensis* cv. Hongshi-2 and non-red-fleshed *A. chinensis* cv. Jinyan and Cuiyu. Their fruit tissues at 80, 90 and 100 DAA were sampled for measurement of total anthocyanin content and for qRT-PCR analysis. As shown in Figure 4, almost no anthocyanin accumulation was detected in non-red-fleshed 'Jinyan' and 'Cuiyu', and the measured expression levels of *AcMYB110*, *AcMYB123*, *AcbHLH42*, *AcF3GT1* and *AcANS* were very low in both the outer and inner pericarp. Similar to the observations in 'Hongyang', a large amount of accumulated anthocyanin and increased expression of *AcMYB110*, *AcMYB123*, *AcbHLH42*, *AcF3GT1* and *AcANS* were detected in the inner pericarp of 'Hongshi-2'. These results further suggest anthocyanin accumulation specifically in the inner pericarp is associated with coordinated action of *AcMYB110*, *AcMYB123*, *AcbHLH42*, *AcF3GT1* and *AcANS* during fruit development and ripening.

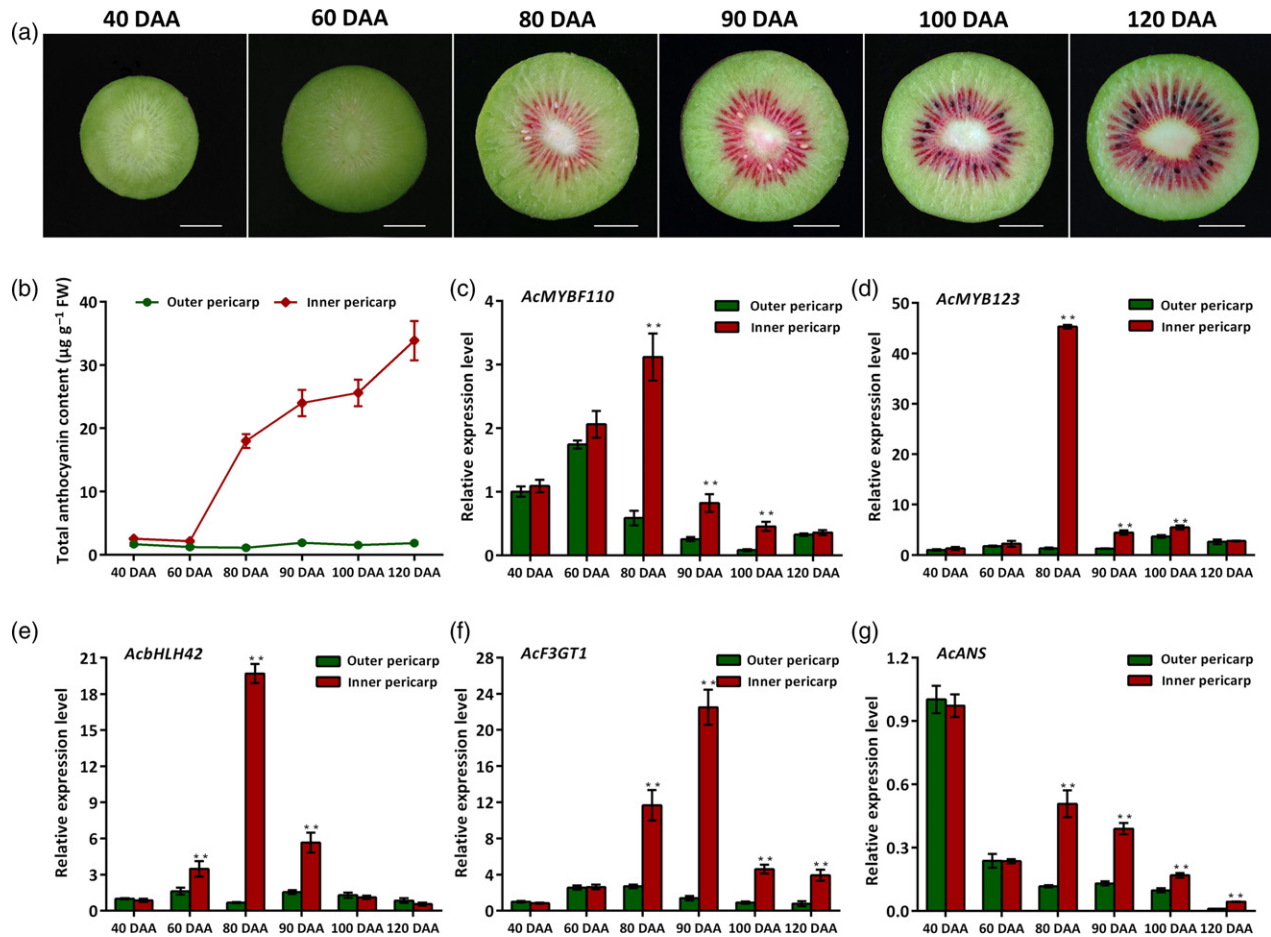


**Figure 3.** Correlation of tissue-specific anthocyanin accumulation with related gene expression.

(a) Transverse sections of red-fleshed *Actinidia chinensis* cv. Hongyang fruits at six developmental stages. Scale bars: 1 cm. (b) Comparison of total anthocyanin content in inner and outer pericarp of Hongyang. (c)–(g) Expression of *AcMYBF110* (c), *AcMYB123* (d), *AcbHLH42* (e), *AcF3GT1* (f) and *AcANS* (g) in inner and outer pericarp of Hongyang fruit at six developmental stages determined by quantitative RT-PCR analysis. \*\*Significant difference at  $P < 0.01$  (one-way ANOVA test). Error bars represent the SD of three replicates. DAA, days after anthesis.

### Downregulation of anthocyanin biosynthesis by RNA-interfering *AcMYB123*, *AcbHLH42*, *AcF3GT1* and *AcANS*

We next employed RNA interference (RNAi) technology to further determine the function of *AcMYB123*, *AcbHLH42*, *AcF3GT1* and *AcANS* in anthocyanin biosynthesis. A transient assay for tracing anthocyanin production was developed in ‘Hongyang’. *Agrobacterium tumefaciens* strain GV3101 harboring gene-specific recombinant plasmids of *35S::AcMYB123-RNAi*, *35S::AcbHLH42-RNAi*, *35S::AcF3GT1-RNAi* and *35S::AcANS-RNAi* was separately injected into the fruit flesh at about 70 DAA. After approximately 20 days, fruit flesh injected with *A. tumefaciens* harboring plasmids containing the gene-specific RNAi hairpins remained green to yellowish, whereas a red color was developed in the inner pericarp of the empty vector-injected fruit (Figure 5a). Anthocyanin biosynthesis was severely inhibited by the RNAi suppression of these genes (Figure 5b). Consistently, qRT-PCR analysis showed that, compared with the control,

there was a significant reduction in transcript levels corresponding to the fruit samples expressing *AcMYB123-RNAi*, *AcbHLH42-RNAi*, *AcF3GT1-RNAi* and *AcANS-RNAi*, respectively (Figure 5c–f). Further analysis showed that RNAi suppression of *AcMYB123* and *AcbHLH42* expression resulted in significantly decreased expression of both *AcF3GT1* and *AcANS* (Figure 5g–j), but no distinct morphological changes in fruit tissues (Figure S9). These results demonstrated that *AcMYB123*, *AcbHLH42*, *AcF3GT1* and *AcANS* are all necessary for conferring anthocyanin accumulation in the inner pericarp of ‘Hongyang’. To determine the specificity of RNAi silencing, the characterized anthocyanin-related MYBs, *AcMYB1/AcMYB10/AcMYB75/AcMYBF110* (Fraser *et al.*, 2013; Man *et al.*, 2015; Li *et al.*, 2017b; Liu *et al.*, 2017) and three additional MYB homologs (accession nos Acc16026/Ach00g270991, Acc22332/Ach19g199471 and Acc26115/Ach23g366791) most closely related to *AcMYB123* (Figures S3 and S4), as well as three bHLH homologs (accession nos Acc31692/Ach28g321841,

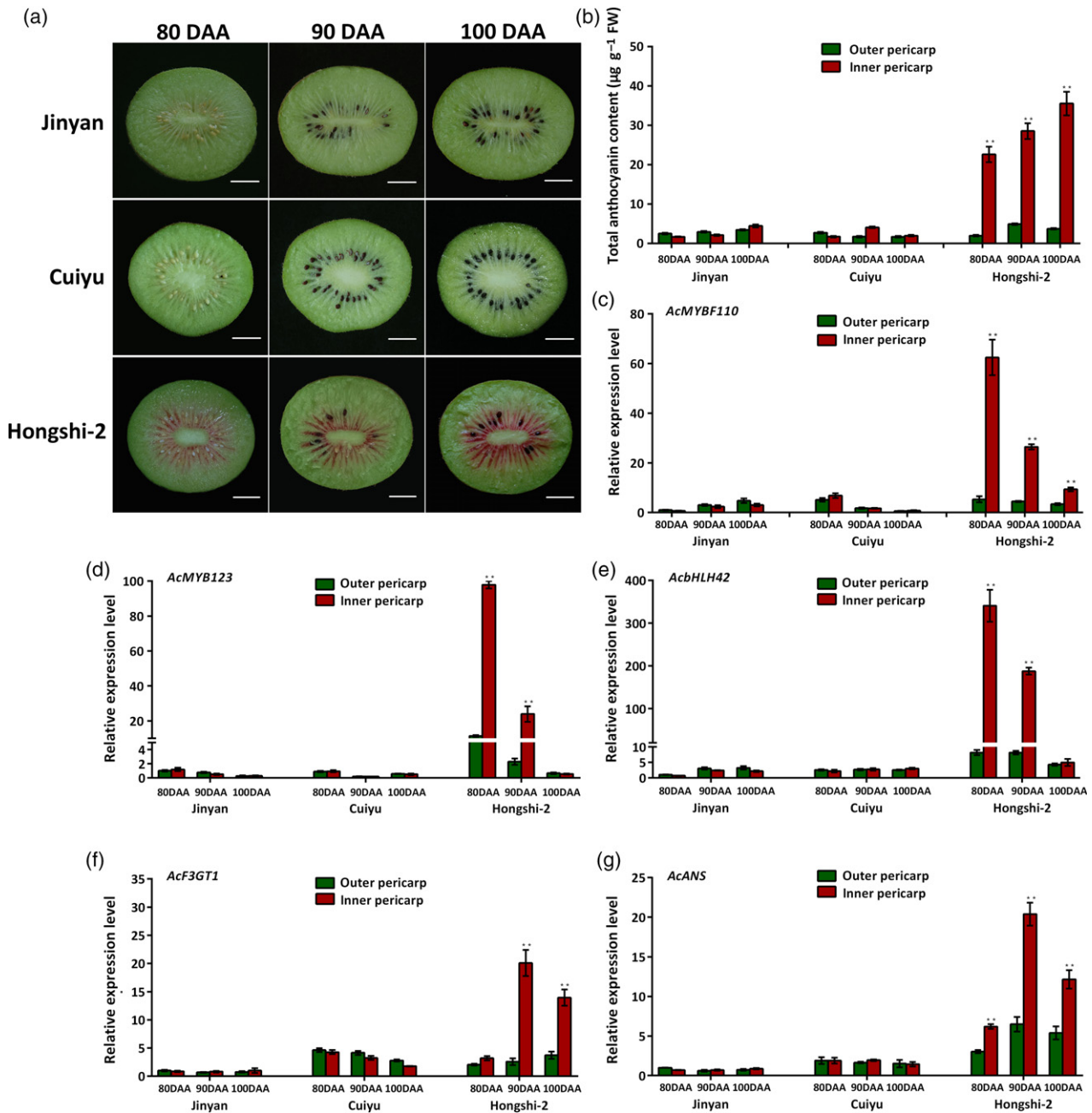


**Figure 4.** Anthocyanin contents and related gene expression in *Actinidia chinensis* cultivars, Jinyan, Cuiyu and Hongshi-2. (a) Bisected fruits of the three cultivars at three developmental stages. Scale bars: 1 cm. (b) Total anthocyanin content in inner and outer pericarp of the three cultivars. (c)–(g) Relative expression levels of *AcMYBF110* (c), *AcMYB123* (d), *AcbHLH42* (e), *AcF3GT1* (f) and *AcANS* (g) in inner and outer pericarp of the three cultivars at three developmental stages determined by quantitative RT-PCR analysis. \*\*Significant difference at  $P < 0.01$  (one-way ANOVA test). Error bars represent the standard deviation of three replicates. DAA, days after anthesis.

Acc20018/Ach18g244201 and Acc09123/Ach08g302211 (Figure S5) most closely related to the *AcbHLH42* were included for the qRT-PCR analyses. Subsequent measurement showed that their expression was nearly unaffected in the RNAi suppressed fruits (Figure S10). These results suggest there was only a low probability of incorrect targeting caused by RNAi suppression and that the observed

phenotypic alterations most likely resulted from downregulation by expression of individual RNAi constructs.

#### **AcMYB123 interacts with AcbHLH42 to activate anthocyanin biosynthesis in *N. tabacum* leaves**

To further verify the function of *AcMYB123* and *AcbHLH42* in anthocyanin biosynthesis, either 35S::*AcMYB123* or

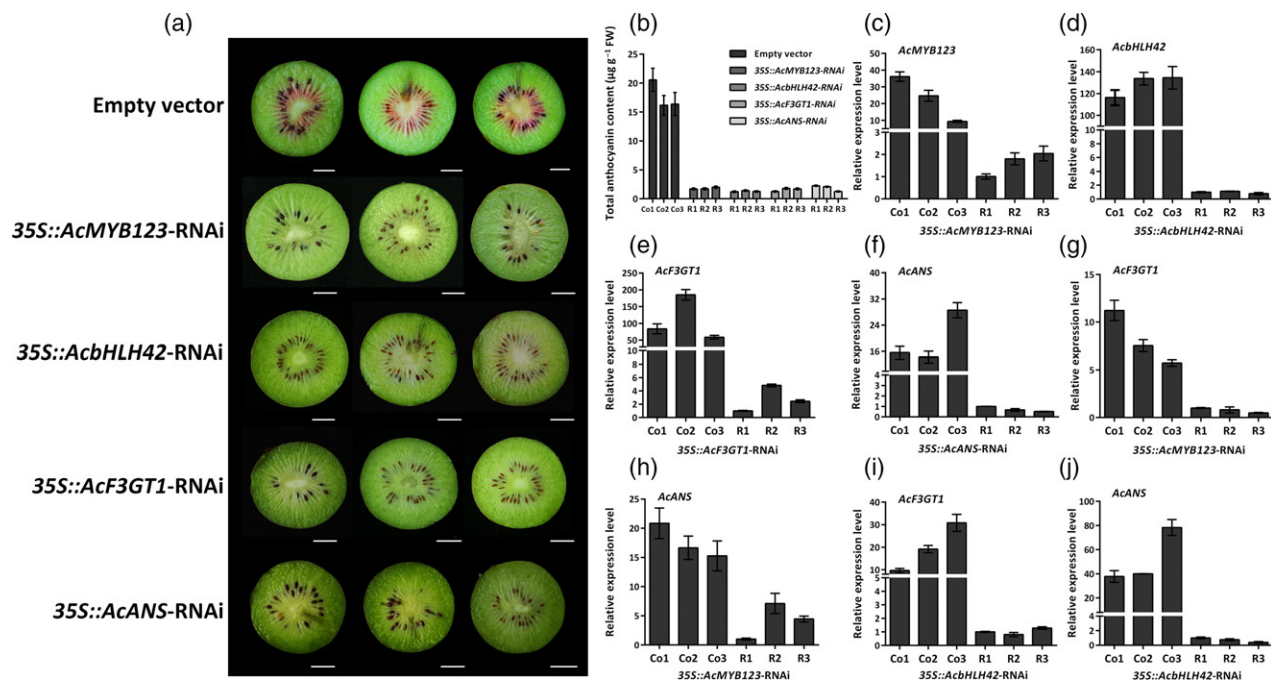


**Figure 5.** Functional characterization of *AcMYB123*, *AcbHLH42*, *AcF3GT1* and *AcANS* in fruit of *Actinidia chinensis* cv. Hongyang using transient RNA interference (RNAi).

*Agrobacterium tumefaciens* GV3101 harboring 35S::*AcMYB123*-RNAi, 35S::*AcbHLH42*-RNAi, 35S::*AcF3GT1*-RNAi or 35S::*AcANS*-RNAi were separately injected into the fruit flesh of Hongyang at 70 days after anthesis. An empty vector (pHB) served as a control.

(a) Bisected fruits at 20 days after the injection. Three replicates are presented.

(b) Total anthocyanin content in the inner pericarp. (c)–(j) Relative expression levels of *AcMYB123* (c), *AcbHLH42* (d), *AcF3GT1* (e) or *AcANS* (f) in the inner pericarp determined by quantitative RT-PCR. An individual RNAi vector group (R) was separately compared with an independent empty vector group (Co). Error bars represent the standard deviation of three replicates.

35S: *AcbHLH42*, or both, were transiently expressed in *N. tabacum* leaves via *A. tumefaciens*-mediated transformation. Infiltration of 35S::*AcMYB110* was used as a positive control (Liu *et al.*, 2017). Interestingly, cellular build-up of anthocyanin was apparently visualized in the microscopic bright-field in the infiltrated leaf samples either expressing *AcMYB110* alone or co-expressing *AcMYB123* and *AcbHLH42*; by contrast the leaf samples separately transformed with 35S::*AcMYB123*, 35S::*AcbHLH42* or empty vector (pHB) failed to accumulate anthocyanin (Figure 6a). We observed anthocyanin accumulation, up to 40 µg g<sup>-1</sup> fresh weight, resulted from cooperative actions of *AcMYB123* and *AcbHLH42* (Figure 6b). Much higher anthocyanin accumulation was observed in the positive control (Figure 6a and b). In addition, in the infiltration patches, substantial transcripts derived from the transformed constructs were detected by the qRT-PCR analysis (Figure 6c–e). Interestingly, the expression of *N. tabacum* structural genes *Nt3GT1* (NM\_001326108.1) (homologous to *AcF3GT1*) and *NtANS* (NM\_001325254.1) (homologous to *AcANS*) was induced by the expression of *AcMYB110* alone or co-expression of *AcMYB123* and *AcbHLH42* (Figure 6f,g).

### Ectopic co-expression of *AcMYB123* and *AcbHLH42* results in elevated anthocyanin accumulation in *A. arguta* and transgenic *Arabidopsis thaliana*

To further demonstrate the function of *AcMYB123* and *AcbHLH42* in other *Actinidia* species, *A. tumefaciens* strain GV3101 harboring the recombinant plasmids of 35S::*AcMYB123* and 35S::*AcbHLH42* were simultaneously injected into fruit flesh of *A. arguta* cv. Baby Star at 100 DAA. Significantly higher levels of anthocyanins were accumulated in the fruits overexpressing *AcMYB123* and *AcbHLH42* compared with the control (Figure 7a,b). The enhanced coloration was observed in some of the infiltrated fruits corresponding to the increased expression levels of *AcMYB123*, *AcbHLH42*, *AcF3GT1* and *AcANS* detected by the qRT-PCR analysis (Figure 7c–f). In addition, to generate transgenic *Arabidopsis* plants expressing either *AcMYB123* or *AcbHLH42* or both, the recombinant vectors 35S::*AcMYB123* and 35S::*AcbHLH42* were separately transformed into *A. thaliana* (Columbia) using the GV3101-mediated floral dipping method (Clough and Bent, 1998). Transgenic lines overexpressing either *AcMYB123* or *AcbHLH42* as well as hybrid lines simultaneously overexpressing both *AcMYB123* and *AcbHLH42* obtained by cross-pollination were subjected to phenotypic evaluation.

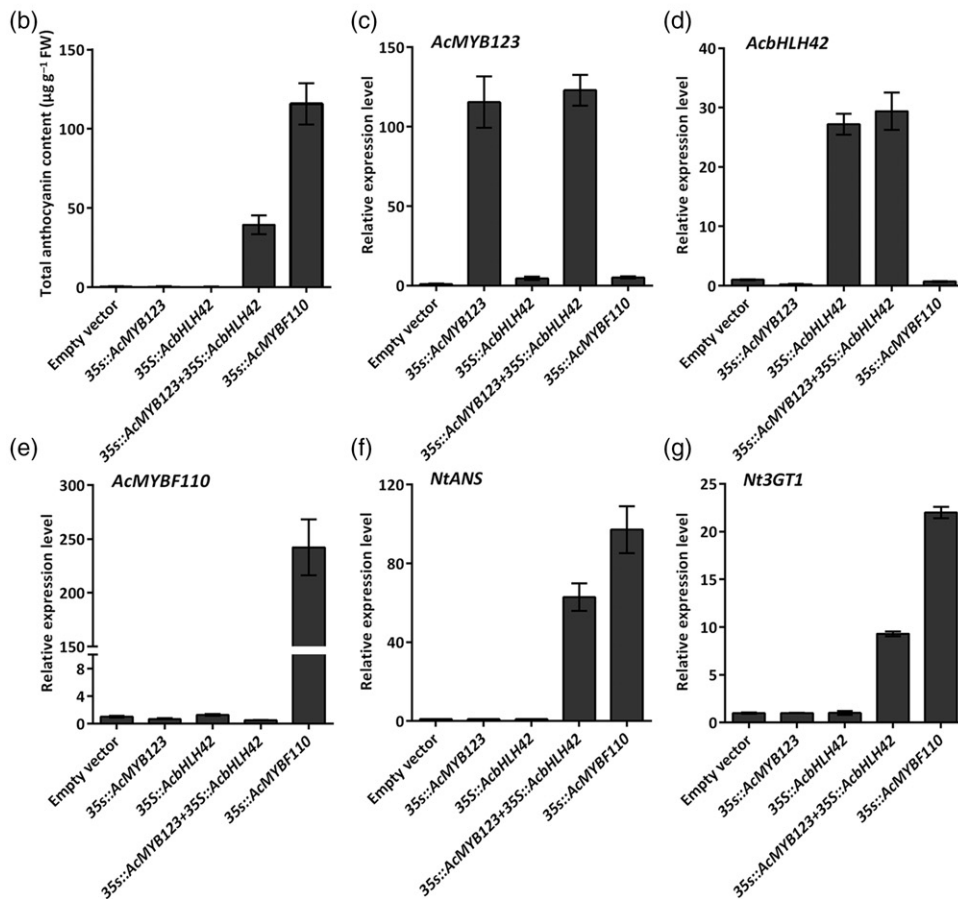
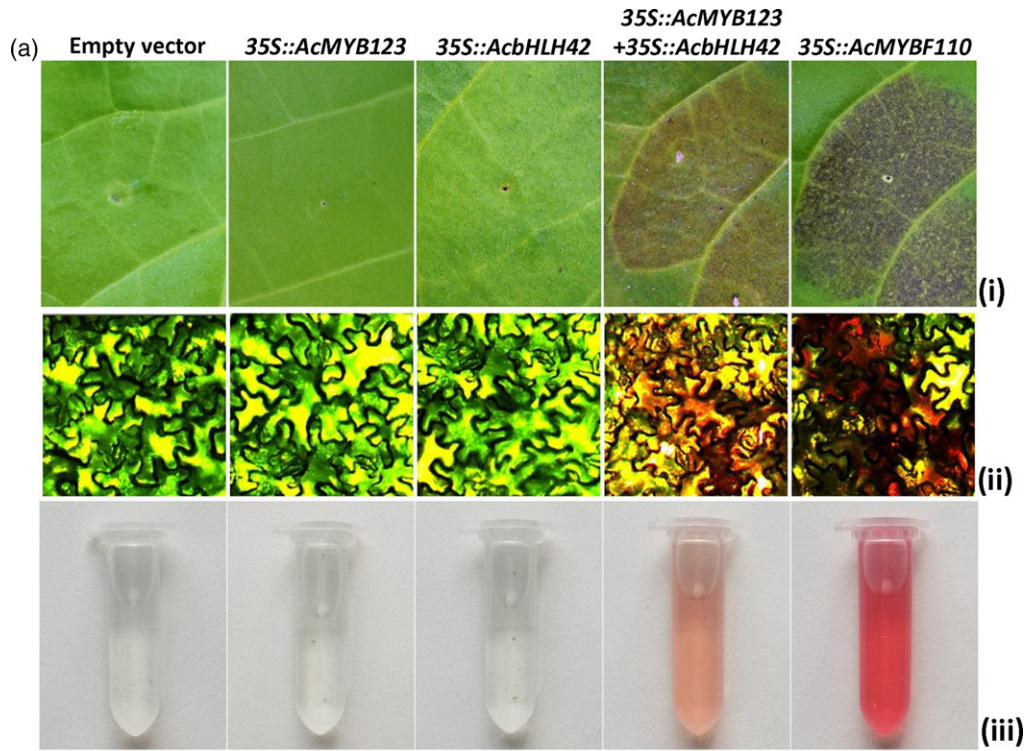


**Figure 6.** The combinatorial action of *AcMYB123* and *AcbHLH42* determines anthocyanin production in transiently expressed *Nicotiana tabacum* leaves. (a) Color changes induced by transiently expressing either *35S::AcMYB123* or *35S::AcbHLH42* alone, or co-expressing *35S::AcMYB123* and *35S::AcbHLH42* in *N. tabacum* leaves (i). *35S::AcMYB110* was used as a positive control. Microscope (20-fold) bright-field images (ii) and fresh extracts from the individual infiltrated patches (iii) showing apparent accumulation of red pigment induced by the combinatorial action of double overexpression. (b) Total anthocyanin content measured in the infiltration patches. Anthocyanin content was determined at 5 days after infiltration. FW, fresh weight. (c)–(g) Quantitative RT-PCR analysis of *AcMYB123* (c), *AcbHLH42* (d), *AcMYB110* (e), *NtANS* (f) and *Nt3GT1* (g) in the infiltration sites. Error bars represent the standard deviation of three replicates.

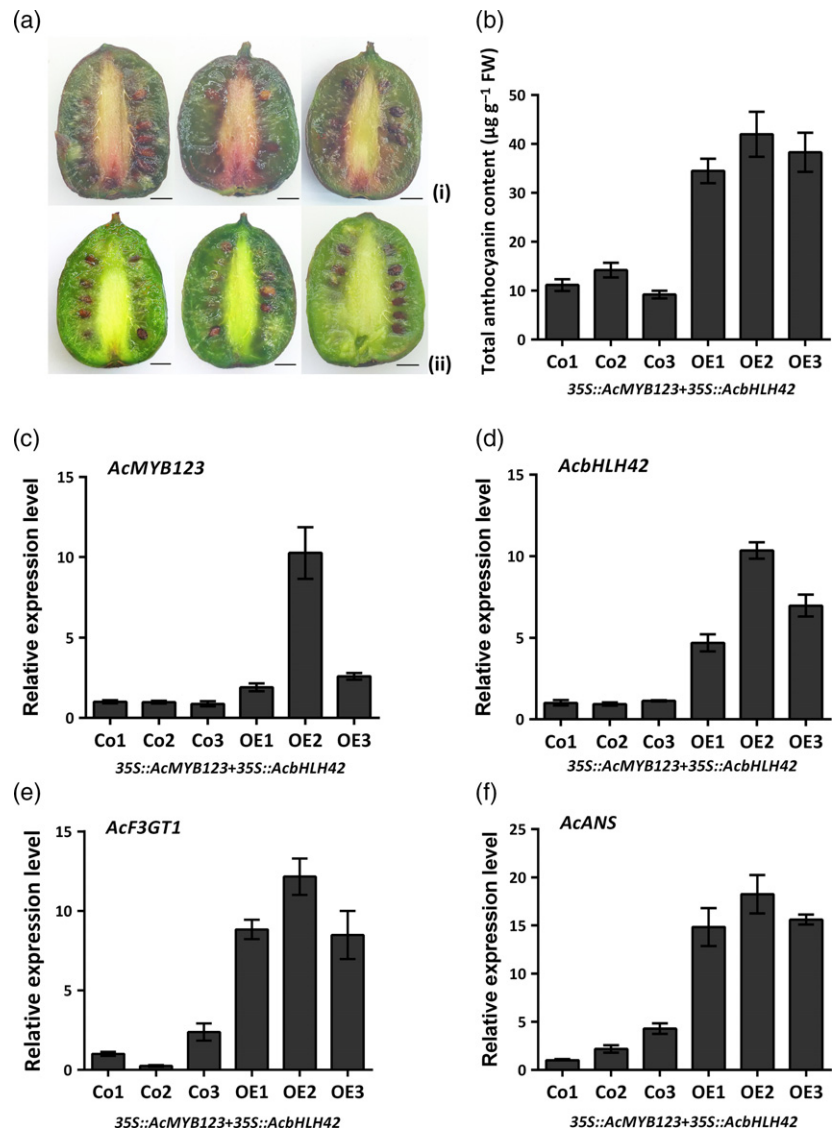
Compared with the wild type, the hybrid transgenic lines co-expressing *AcMYB123* and *AcbHLH42* showed significantly enhanced anthocyanin accumulation in 8-day-old seedlings, although transgenic seedlings expressing either *AcMYB123* or *AcbHLH42* alone also displayed visible, but not significant, color change (Figure 8a,b). The transgene expression corresponding to the increased anthocyanin accumulation was validated by semi-quantitative RT-PCR analysis (Figure 8c). Interestingly, the expression of two *Arabidopsis* structural genes, *AtUF3GT* (AT5G54060.1)

(homologous to *AcF3GT1*) and *AtANS* (AT4G22880.1), was more or less enhanced by expressing either *AcMYB123* or *AcbHLH42* alone or both (Figure 8d,e).

**DISCUSSION**

The spatiotemporal regulation of anthocyanin biosynthesis has been well documented in plants and involves an MBW complex consisting of an R2R3 MYB, a bHLH and a WD40 protein. The main objective of this study was to identify regulators of anthocyanin biosynthesis in *Actinidia* fruit.

**Figure 7.** Anthocyanin production induced by ectopic co-expression of *AcMYB123* and *AcbHLH42* in *Actinidia arguta* cv. Baby star. *Agrobacterium tumefaciens* strains GV3101 harboring the recombinant plasmids of *35S::AcMYB123* and *35S::AcbHLH42* were injected into fruit flesh of *A. arguta* cv. Baby star at 100 days after anthesis. An empty vector (pHB) was used as a control (Co). (a) Bisected fruits at 5 days after injection of the vector co-expressing *AcMYB123* and *AcbHLH42* (i) or the empty vector (ii). Scale bars: 0.5 cm. (b) Anthocyanin content in the treated fruit tissues. (c)–(f) Relative expression levels of *AcMYB123* (c), *AcbHLH42* (d), *AcF3GT1* (e) or *AcANS* (f) in the treated fruit tissues determined by quantitative RT-PCR analysis. Error bars indicate the standard deviation of three replicates.



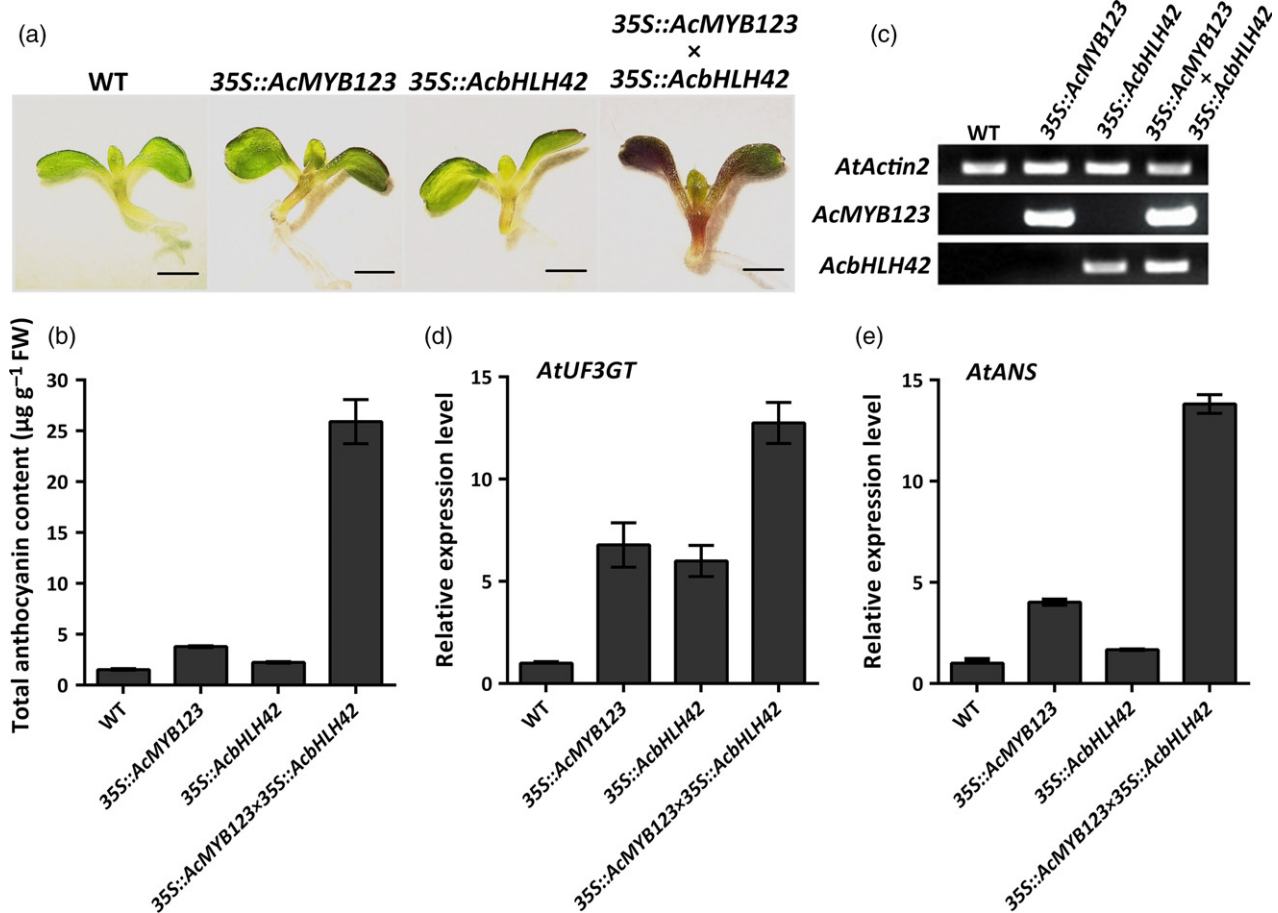


**Figure 8.** Anthocyanin production induced by ectopic co-expression of AcMYB123 and AcbHLH42 in *Arabidopsis thaliana*.

(a) Eight-day-old seedlings of the wild type (WT), transgenic lines overexpressing *AcMYB123* or *AcbHLH42* and hybrid transgenic lines overexpressing both *AcMYB123* and *AcbHLH42*. Scale bars: 1 mm.

(b) Total anthocyanin content measured in 8-day-old seedling leaves of WT and transgenic lines. FW, fresh weight.

(c) Transgene expression detected by semi-quantitative RT-PCR analysis. *AtActin2* served as an internal reference.

(d), (e) Relative expression levels of *AtUF3GT* and *AtANS* detected by quantitative RT-PCR analysis using 8-day-old seedling leaves from different genotypes. Error bars indicate standard deviation of three replicates.

For this purpose, transcriptomic, molecular and biochemical approaches were employed. The results presented here demonstrate that a kiwifruit R2R3 MYB regulator (AcMYB123) and its interacting bHLH protein (AcbHLH42) from the Illf subgroup are necessary for anthocyanin production specifically in the inner pericarp of *A. chinensis* cv. Hongyang.

#### AcMYB123 and AcbHLH42 are highly homologous to TT2 and TT8, respectively, in *Arabidopsis*

In various plant species, R2R3 MYB TFs interact with bHLH proteins from the Illf subgroup to regulate anthocyanin/proanthocyanidin biosynthesis (Xu *et al.*, 2015). In plants, the first characterized anthocyanin-associated MYB-related protein, C1, is a R2R3 MYB TF from maize (*Zea mays*) (Cone *et al.*, 1986; Paz-Ares *et al.*, 1987). The R2R3-MYB TFs contain two sets of imperfect repeats (R2 and R3), each

containing three alpha-helices forming a helix–turn–helix motif (Du *et al.*, 2009). The interactions involve the MYB R3 repeat and the N-terminal MYB-interacting region (MIR) of the Illf subgroup bHLH proteins that contain a conserved arginine residue. Here we show AcMYB123 specifies a typical R2R3-MYB domain protein containing an R3 repeat with a conserved motif (D/E)LX<sub>2</sub>(R-K)X<sub>3</sub>LX<sub>6</sub>LX<sub>3</sub>R that may confer the interacting ability with its bHLH partner of kiwifruit (AcbHLH42) demonstrated by the BiFC and Co-IP assays (Figure 2). Interestingly, phylogenetic analysis (Figure S3) of the R2R3-MYB domain of AcMYB123 and the related MYB family members from various plant species indicates that AcMYB123 is more closely related to *Arabidopsis* TT2/AtMYB123, specifically required for regulating proanthocyanidin biosynthesis (Nesi *et al.*, 2001; Baudry *et al.*, 2004), than to anthocyanin regulators in both monocots and dicots, such as *Arabidopsis* AtPAP1/PAP2

(Borevitz *et al.*, 2000), maize C1 (Paz-Ares *et al.*, 1987) and to other kiwifruit anthocyanin-related MYB proteins (Fraser *et al.*, 2013; Man *et al.*, 2015; Li *et al.*, 2017a,b; Liu *et al.*, 2017). Consistently, AcMYB123 is highly homologous to TT2-like R2R3-MYBs from strawberry (*Fragaria ananassa*) (FaMYB9/FaMYB11) and peach (*Prunus persica*) (Peace) (Figure S3) in anthocyanin or proanthocyanidin production (Nesi *et al.*, 2001; Schaart *et al.*, 2013; Uematsu *et al.*, 2014). Meanwhile, as for maize Lc/R, the founding member of the plant bHLH family involved in tissue-specific anthocyanin production (Chandler, 1989; Ludwig *et al.*, 1989), AcbHLH42 also encodes an R/B-like bHLH protein of the subgroup IIIf containing an N-terminal MYB interaction region (MIR) and C-terminal bHLH domain required for DNA binding (Figure S5). Intriguingly, phylogenetic analysis indicates AcbHLH42 is most closely related to Arabidopsis TT8/AtbHLH042, which specifically regulates proanthocyanidin biosynthesis (Nesi *et al.*, 2000; Schaart *et al.*, 2013). Together, these analyses implicate that AcMYB123 and AcbHLH42 encode the closest flavonoid-related regulatory proteins orthologous to TT2/AtMYB123 and TT8/AtbHLH042, respectively, in Arabidopsis. Actually, TT2/TT8 has been initially shown to play a major role in specific accumulation of proanthocyanidin in the innermost cell layer of Arabidopsis seed coat (Nesi *et al.*, 2000, 2001; Baudry *et al.*, 2004). Unlike seed-specific proanthocyanidin accumulation regulated by TT2/TT8 in Arabidopsis, in the red-centered kiwifruit cultivars anthocyanin appears to accumulate specifically in the inner pericarp flesh that encompasses the developing seeds (Figures 3a and 4a). Similar flavonoid-accumulating regulatory gene(s) structurally orthologous to TT2/TT8 have been characterized in strawberry, showing that fruit-expressed FaMYB9/FaMYB11 and FabHLH3 are able to complement the *tt2-1* and *tt8-3 transparent testa* mutants with modified seed pigmentation in Arabidopsis (Schaart *et al.*, 2013). In peach a TT2-like gene PEACE (peach anthocyanin colour enhancement) is involved in regulating accumulation of anthocyanin instead of proanthocyanidin in petal pigment (Uematsu *et al.*, 2014). In *Petunia* AN2/AN1 participates in regulating anthocyanin pigmentation in the flower petals (Vetten *et al.*, 1997; Quattrocchio *et al.*, 1998). In apple the TT2-like proanthocyanidin-specific TF MdMYBPA1 initiates anthocyanin synthesis under low-temperature conditions (Wang *et al.*, 2018). These observations indicate that transcriptional regulation of the flavonoid pathway in different plant species involves highly structurally conserved MYB- and bHLH-related proteins.

#### **Combinatorial action of AcMYB123 and AcbHLH42 is essential for target structural gene expression and anthocyanin production**

Our results strongly suggest that the AcMYB123 activity is tightly linked to the presence of AcbHLH42. Lack of either

AcMYB123 or AcbHLH42 means that target structural gene expression and anthocyanin biosynthesis cannot be activated (Figures 1, 6–8). These findings highlight the importance of the interaction specificity between the cooperative partners of MYB- and bHLH-related proteins in regulating flavonoid metabolism. Such interacting partners dedicated to flavonoid production have been previously described in several plant species. For example, in Arabidopsis, TT2/AtMYB123 was able to induce the ectopic expression of *BANYULS* encoding an anthocyanidin reductase (Devic *et al.*, 1999) in young seedlings and roots in the presence of a functional TT8/AtbHLH042 protein (Nesi *et al.*, 2001). In maize, the presence of an amino acid motif in the R3 region determines the binding specificity of the R2R3 MYB to the bHLH partner and confers the ability of C1 to interact with the bHLH protein R that is specifically responsible for triggering the activation of target gene *ZmBz1* (Grotewold *et al.*, 2000; Zimmermann *et al.*, 2004). MYB or bHLH protein can interact with multiple bHLH or MYB partners to specify flavonoid accumulation in diverse plant tissues. In the case of Arabidopsis, at least four MBW complexes, namely TT2-TT8/GL3/EGL3-TTG1 and MYB5-TT8-TTG1, with partially overlapping functions, were identified in regulating specific accumulation of proanthocyanidin in the innermost cell layer of the seed coat, while in vegetative tissues anthocyanin biosynthesis is also regulated by different sets of MBW complexes (PAP)1–4, GL3/EGL3/TT8 and TTG1 (Xu *et al.*, 2015). Similarly, two MBW complexes (FaMYB9/FaMYB11-FabHLH3-FaTTG1) highly homologous to the Arabidopsis TT2-TT8-TTG1 complex were shown to regulate flavonoid biosynthesis in strawberry fruit (Schaart *et al.*, 2013). It seems likely that the MBW complex constitutes different classes of MYBs and bHLHs with specific functions in regulating the transcription of the flavonoid pathway. Moreover, hierarchical and feedback regulations have been established for the MBW complex for regulation of flavonoid biosynthesis. R3-MYB or R2R3-MYB repressors have been proposed to assert their repressive function through competition for bHLH partners with R2R3-MYB activators that activate expression of anthocyanin genes (Koes *et al.*, 2005; Albert *et al.*, 2014). The key bHLH factor TT8, including its homologs as well as the MYB repressors, were shown to be transcriptionally activated by MBW complexes that include the bHLH component itself (Baudry *et al.*, 2004; Albert *et al.*, 2014). These suggest that the specificity of functions amongst similar TFs, or the involvement of distinct MYB protein classes with opposite function, would allow for fine-tuned regulation of flavonoid metabolism in response to developmental or environmental cues through different combinations of TFs within the MBW complex. In addition to AcMYB123 and AcbHLH42 characterized in this study, we believe additional MYB- and bHLH-interacting pairs might participate

in the regulation of anthocyanin accumulation in the inner pericarp of kiwifruit. Actually, we found that previously characterized anthocyanin-related MYBs (*AcMYB1*, *AcMYB10*, *AcMYB75* and *AcMYBF110*) (Figure S4) were derived from the same locus (Acc00493.1) (Pilkington *et al.*, 2018), suggesting that this MYB gene is frequently identified as an important regulator in anthocyanin pigmentation in diverse kiwifruit cultivars (Fraser *et al.*, 2013; Man *et al.*, 2015; Li *et al.*, 2017b; Liu *et al.*, 2017). Surprisingly, physical interaction between *AcMYBF110* and *AcbHLH42* was clearly visualized using BiFC and Co-IP assays (Figure S7), and substantially enhanced anthocyanin pigments were produced by co-expressing *AcMYBF110* and *AcbHLH42* compared with expressing *AcMYBF110* alone in tobacco leaves (Figure S11), suggesting that *AcMYBF110* and *AcbHLH42* can physically interact with each other and form a complex to accelerate target gene expression. Phylogenetic analysis indicates that *AcMYBF110* is the most closely related ortholog of Arabidopsis PAP1 (Figure S3), an R2R3 MYB gene that is able to interact with TT8 and TTG1 to form a MBW complex involved in the regulation of production of anthocyanin pigment in vegetative tissues (Baudry *et al.*, 2006; Gonzalez *et al.*, 2008). Since substantially higher expression levels of *AcMYBF110*, *AcMYB123* and *AcbHLH42* were detected in the inner than the outer pericarp during anthocyanin pigmentation (Figures 3 and 4), we could postulate that at least two MBW complexes (*AcMYB123/AcbHLH42* and *AcMYBF110/AcbHLH42*) with partially overlapping functions might be involved in the regulation of specific accumulation of anthocyanin in the inner pericarp of red-centered kiwifruits. According to the released kiwifruit genomes (Huang *et al.*, 2013; Pilkington *et al.*, 2018), *AcMYBF110* and *AcMYB123* localize to chromosomes 1 and 24, respectively, and appear to be under the control of different *cis*-regulatory elements (Figure S12) as indicated by their distinct expression patterns throughout fruit development (Figure 3c,d). Moreover, *AcMYB5-1* and *AcMYBA1-1* (Li *et al.*, 2017a) are expressed throughout fruit development with a pattern similar to *AcMYB123* (Figures 3d and S13a,b) but their bHLH partners are unknown. Intriguingly, the expression of *AcMYB5-1* and *AcMYBA1-1* was largely unaffected, in contrast to that of *AcMYBF110/AcMYB75/AcMYB1/AcMYB10* that showed enhanced transcription by ectopic expression of *AcMYB123* and *AcbHLH42* in fruit flesh of *A. arguta* cv. Baby Star (Figure 7; Figure S14), implicating *AcMYB123/AcbHLH42* as upstream regulators of *AcMYBF110* (*AcMYB75/AcMYB1/AcMYB10*) with regard to anthocyanin accumulation specifically in the inner pericarp of kiwifruit. To test this hypothesis, we isolated the promoter sequences of *AcMYBF110*, *AcMYB123* and *AcbHLH42*, which were subsequently constructed upstream of the GUS reporter gene. These individual constructs were then

co-expressed with 35S::*AcMYBF110*, 35S::*AcMYB123* or 35S::*AcbHLH42* alone or in combination in tobacco leaves. As shown in Figure S15, none of them could activate the expression of the other, suggesting that the *AcMYBF110* promoter is not the direct target of *AcMYB123/AcbHLH42* (Figure S15). Our transcriptome profiling data also show that elevated expression of four MYBs (*AcMYB44*, *AcMYB3R-1*, *AcMYB3R-5* and *AcMYBPA1*) and two bHLHs (*AcGL3* and *AcEGL3*) is associated with the presence of anthocyanin in the inner pericarp (Table S1, Figure S2), but their interacting partners or their functional properties for anthocyanin metabolism, if any, remain to be identified.

### Both *AcMYB123* and *AcbHLH42* target late anthocyanin biosynthesis genes

Here we showed that two late anthocyanin biosynthesis genes in kiwifruit, *AcANS* encoding an anthocyanidin synthase and *AcF3GT1* encoding a flavonoid 3-O-glucosyltransferase, were differentially expressed between the inner and outer pericarp and regulated by *AcMYB123* and *AcbHLH42*. Indeed, the first downstream enzyme, DFR (GenBank accession no. KF157393), the key branch point gene within the flavonoid pathway between flavonols and anthocyanins/proanthocyanidins, was excluded for the tissue-specific regulation of anthocyanin biosynthesis although its expression in outer pericarp was slightly higher, but not significantly so, than in inner pericarp throughout developmental stages (Figure S16). Our data demonstrated that the elevated expression of both *AcANS* and *AcF3GT1* is consistent with the upregulation of *AcMYB123/AcbHLH42* and anthocyanin accumulation in the inner pericarp of 'Hongyang' (Figures 3 and 4). Enhanced expression of both *AcANS* and *AcF3GT1* or their orthologous genes leading to anthocyanin production was induced by ectopic expression of both *AcMYB123* and *AcbHLH42* using transient assays in tobacco leaves (Figure 6) or *A. arguta* fruits (Figure 7) and using stable transgenic Arabidopsis (Figure 8). By contrast, RNAi repression of either *AcMYB123* or *AcbHLH42* in fruits of 'Hongyang' resulted in decreased expression of both *AcANS* and *AcF3GT1* and significantly reduced production of anthocyanins (Figure 5). Previous investigations also showed that the expression of *AcF3GT1* is correlated with anthocyanin pigmentation in red tissues and its transcription can be activated by co-expressing Arabidopsis PAP1 (a R2R3-MYB member) and TT8/*AtbHLH042* in fruits of kiwifruit (Montefiori *et al.*, 2011). The *F3GT1* gene encodes the key enzyme regulating anthocyanin production, and its expression has been shown to be highly regulated in the anthocyanin biosynthetic pathway (Griesser *et al.*, 2008; Cutanda-Perez *et al.*, 2009). We searched for *cis*-regulatory elements in the promoters of *AcF3GT1*, *AtUF3GT* and *Nt3GT1* based on the PLACE (Plant *cis*-Acting Regulatory

DNA Elements) database (Higo *et al.*, 1999) and found putative MYB-binding sites (CNGTTR3 or [A/C]CC[A/T]A[A/C]) and bHLH-binding sites (CANNTG/CACGTG) in all their promoters (Xu *et al.*, 2015) (Figure S17). Similar analysis showed that the same *cis*-elements exist in the promoters of *AcANS*, *AtANS* and *NtANS* (Figure S17). These analyses suggest that activation of *AcANS* and *AcF3GT1* expression may be mediated by combinatorial action of *AcMYB123* and *AcbHLH42*, presumably by interaction with these conserved *cis*-elements. In addition, because *AcMYB123/AcbHLH42* is closely related to *AtTT2/AtTT8*, which is involved in specific proanthocyanidin (PA) synthesis, we also investigated the possibility of PA biosynthesis being regulated by *AcMYB123/AcbHLH42*. Indeed, PA derivatives (such as catechin, epicatechin and procyanidin) have been detected in the phenolic composition of kiwifruit juice by HPLC analysis (Dawes and Keene, 1999). We additionally conducted qRT-PCR and HPLC assays and showed that an *Actinidia ANR* (anthocyanidin reductase) homolog (*Acc17426/Ach15g111861*) and an *LAR* (leucoanthocyanidin reductase) homolog (*Acc32899/Ach29g221841*) were bona fide expressed (Figure S18a,b) and a small amount of epicatechin was accumulated in the fruit flesh (Figure S18c). Nevertheless, these PA-related genes showed relatively high expression levels at early developmental stages and their expression declined sharply during anthocyanin pigmentation, almost displaying the opposite expression patterns to that of *AcMYB123/AcbHLH42* (Figure 3d,e) throughout fruit development. This indicates that involvement of *AcMYB123/AcbHLH42* in the regulation of PA biosynthesis is unlikely in *Actinidia* fruit. In any case, future work will have to integrate the important role of *AcMYB123/AcbHLH42* or *AcMYBF110/AcbHLH42* complex in the control and specificity of PA-related gene expression in both vegetative and reproductive tissues.

#### Spatiotemporal expression of *AcMYBF110*, *AcMYB123* and *AcbHLH42*

Our data and previous investigations demonstrated that, during fruit development and in different fruit tissues, *AcMYBF110* (*AcMYB75/AcMYB1/AcMYB10*), *AcMYB123* and *AcbHLH42* (Figure 3) showed the strongest correlation with anthocyanin content, being highly expressed in a specific tissue (inner pericarp of red-centered fruit) and at specific time points, suggesting that the expression of *AcMYBF110/AcMYB123* and *AcbHLH42* may be regulated spatiotemporally (Fraser *et al.*, 2013; Man *et al.*, 2015; Li *et al.*, 2017b; Liu *et al.*, 2017). In addition, several R2R3-MYB TFs from different plant species have been shown to be involved in the spatiotemporal regulation of anthocyanin metabolism. For instance, *AcMYB110* from kiwifruit was highly expressed at early developmental stages of red petals and is responsible for the accumulation of anthocyanin pigment in red petals but not in other flower tissues

or mature fruit (Fraser *et al.*, 2013). Its ectopic expression in tobacco showed a strong activation of the anthocyanin pathway (Montefiori *et al.*, 2015). These findings indicate that the expression of *AcMYBF110/AcMYB123*, *AcbHLH42* and other anthocyanin-related regulators might be fine-tuned and modulated by higher hierarchical factors, such as other TFs, post-translational modification, developmental clues and environmental stimuli suggested by recent investigations (Wu *et al.*, 2014; Xu *et al.*, 2015). However, the factors regulating expression of *AcMYBF110/AcMYB123-AcbHLH42* for anthocyanin production in the inner pericarp of red-centered kiwifruit cultivars remain to be investigated.

In summary, our results reveal that *AcMYB123* and *AcbHLH42* are interacting partners and highly conserved structurally and functionally with Arabidopsis TT2 and TT8, respectively, and play a pivotal role in anthocyanin biosynthesis by activating the transcription of *AcANS* and *AcF3GT1*. We also provide evidence to show that *AcbHLH42* physically interacts with *AcMYBF110*, the most closely related ortholog of Arabidopsis PAP1, to participate in regulation of specific anthocyanin synthesis. The data presented here support, at least partially, the hypothesis that the transcriptional regulation of anthocyanin biosynthesis involves an MBW complex consisting of an R2R3 MYB, a bHLH and a WD40 protein (Baudry *et al.*, 2004). But unfortunately, a corresponding WD40 protein putatively interacting with *AcMYB123* and *AcbHLH42* was not identified from our transcriptome profiling analysis. Previous analyses indicated the *Acc03242/Ach03g045741* from the genome of kiwifruit 'Hongyang' (Huang *et al.*, 2013; Yue *et al.*, 2015; Pilkington *et al.*, 2018) encodes a WD40 protein that is highly homologous to Arabidopsis TTG1, a well-characterized WD40 protein involved in anthocyanin metabolism (Walker *et al.*, 1999). This WD40 homolog from kiwifruit was previously shown to be expressed constitutively throughout fruit development (Tang *et al.*, 2016). Here we additionally demonstrated that there was no significant difference in expression levels of *Acc03242/Ach03g045741* between inner and outer pericarp using qRT-PCR analysis (Figure S19). We also found by Co-IP analysis that neither *AcMYB123* nor *AcbHLH42* could interact with *Acc03242/Ach03g045741* (Figure S20). Future work will be needed to identify the corresponding WD40 protein candidates.

## EXPERIMENTAL PROCEDURES

### Plant materials

*Actinidia chinensis* cvs Hongyang, Hongshi-2, Jinyan and Cuiyu were grown in the experimental station of Sichuan University, Sichuan Province, China. The inner and outer pericarp of fruits at different developmental stages (40, 60, 80, 90, 100, and 120 DAA) were collected with seeds removed. The sampled tissues with three biological replicates were immediately frozen in liquid nitrogen and stored at  $-80^{\circ}\text{C}$ . Arabidopsis (Columbia) and tobacco

plants (*N. benthamiana* and *N. tabacum*) were grown in a greenhouse under a 16-h light/8-h dark photoperiod at 25°C.

### Differential gene expression analysis by RNA-Seq

Total RNA was isolated using BIOFIT Reagent (BIOFIT, China, [www.biofit.com.cn/](http://www.biofit.com.cn/)) followed by treatment with RNase-free DNase I according to the manufacturer's protocols. The quality of RNA was checked using agarose gel electrophoresis, and quantities were determined using Agilent 2100 Bioanalyzer (Agilent, <http://www.agilent.com/>) and NanoDrop ND-1000 Spectrophotometer (<http://www.thermofisher.com/>). Complementary DNA was then synthesized from 1 µg of total RNA using HiFiScript Quick gDNA Removal cDNA synthesis (CW BIO, <http://www.cwbiotech.com/>). Four RNA-Seq libraries (two for the outer pericarp and two for the inner pericarp of fruits at 90 DAA) were constructed and sequenced on an Illumina HiSeq 2000 system following the manufacturer's instructions (Illumina, <http://www.illumina.com/>). The raw RNA-Seq data have been deposited in the NCBI sequence read archive under the accession number GSE108099.

The adaptor and low-quality sequences were removed from raw RNA-Seq reads using Trimmomatic (Bolger *et al.*, 2014). The cleaned RNA-Seq reads were aligned to the Hongyang genome using STAR (Dobin and Gingeras, 2016). Fragments per kilobase of exon model per million mapped fragments (FPKM) values of each gene were calculated, and DEGs between inner and outer fruit pericarp of Hongyang were identified using Cufflinks (Trapnell *et al.*, 2010). Raw *P*-values were corrected for multiple testing using the Benjamini–Hochberg adjustment (Benjamini and Hochberg, 1995). Genes with a fold change  $\geq 2$  and an adjusted *P*-value  $< 0.01$  were considered to be differentially expressed. Pearson's correlation coefficient *r* was calculated to evaluate the correlation of biological replicates (Schulze *et al.*, 2012).

### Real-time quantitative PCR

Real-time quantitative PCR was carried out in a total volume of 20 µl containing 10 µl of Ultra SYBR Mixture (CW BIO), 0.4 µM primers (listed in Table S2) and 6 µl of 1:15 diluted cDNA. Thermal cycling consisted of a hold at 95°C for 10 min followed by 40 cycles of 95°C for 15 sec and 60°C for 1 min. Melting curve analysis was performed ranging from 60 to 95°C, and PCR products were separated on an agarose gel and sequenced to confirm the specificity of the PCR reaction and verify the accuracy of the amplification. Each sample was amplified in triplicate, and all PCR reactions were performed on the StepOne Real-time PCR System (Applied Biosystem, <http://www.thermofisher.com/>). The transcript expression levels were quantified by the  $2^{-\Delta\Delta CT}$  method (Livak and Schmittgen, 2001) with *AcActin1* (EF063572) (Li *et al.*, 2010), *NtUBQ* (XM\_016648389.1) (Nakatsuka *et al.*, 2012) and *AtActin2* (AK063598) (Xie *et al.*, 2016) as the endogenous controls.

### Anthocyanin determination

A HPLC assay was employed to determine the anthocyanin contents in fruit tissues. Pericarp tissues collected from the *A. chinensis* cultivars or the transiently transformed *A. arguta* fruits were ground into fine powder with liquid nitrogen. Ten grams of powder was used for anthocyanin extraction according to the previously described procedure (Montefiori *et al.*, 2005). The filtered extracts were used for the HPLC assay on an Agilent 1200 Series HPLC System (Agilent) with C18 Aqua column (150 mm  $\times$  4.6 mm i.d., 3 µm; Phenomenex, <http://www.phenomenex.com/>) and photodiode array detector. The injection volume was 20 µl. Separation was achieved with a binary solvent system, 5% aqueous formic

acid (v/v) and acetonitrile (Montefiori *et al.*, 2005; Comeskey *et al.*, 2009). Anthocyanin was monitored at 530 nm. Chromatographic peaks were identified and quantified by comparison with an authenticated standard of cyanidin chloride (CAS no. 528-58-5, ChromaDex, <http://www.chromadex.com/>).

The total anthocyanin content in the tobacco leaves or the Arabidopsis seedlings was extracted in 30–50% acid methanol and determined using the pH differential method described previously (Niu *et al.*, 2010a); this involved measuring the absorbance at 510 and 700 nm using UV–vis spectrophotometer (SHIMADZU UV-2450, <http://www.shimadzu.com/>). At least three biological replications were performed.

### Gene cloning

Five MYB homologs, *AcMYB44* (Acc23779/Ach21g298761), *AcMYB3R-1* (Acc19986/Ach00g380251), *AcMYB3R-5* (Acc16851/Ach15g109311), *AcMYBPA1* (Acc08348/Ach08g104391) and *AcMYB123* (Acc28234/Ach24g242211), as well as three bHLH homologs, *AcbHLH42* (Acc19563/Ach17g348381), *AcGL3* (Acc20018/Ach18g244201) and *AcEGL3* (Acc20202/Ach18g071731), were cloned from Hongyang and inserted into the pHB vector (Yu *et al.*, 2000) using primers shown in Table S2 to generate 35S::*AcMYBs/AcbHLHs* constructs.

### Agrobacterium tumefaciens-mediated transient expression and GUS assays

To construct *pAcF3GT1::GUS*, the *AcF3GT1* promoter, 1867 bp upstream of the coding region of *AcF3GT1* (Acc20131/Ach18g209671), was isolated from Hongyang and cloned into the pBI121 vector to replace the CaMV35S promoter which is upstream of the GUS reporter (Chen *et al.*, 2003). Similarly, the *AcANS* promoter, 1675 bp upstream of the coding region of *AcANS* (Acc28876/Ach00g361621), was isolated from Hongyang and cloned into the pBI121 vector to replace the CaMV35S promoter to construct *pAcANS::GUS*. *pAcF3GT1::GUS* and 35S::*AcMYB/AcbHLH* (different combinations of *AcMYB* and *AcbHLH* pairs) were independently transformed into *A. tumefaciens* strain GV3101, to be used for *A. tumefaciens*-mediated transient expression as described previously (Yang *et al.*, 2000). Six-week-old *N. benthamiana* leaves were infiltrated with either *pAcF3GT1::GUS/35S::AcMYBs/35S::AcbHLHs* alone or individual combinations of 35S::*AcMYB/35S::AcbHLH* pairs, and the constitutive expression construct 35S::GUS served as the positive control. In addition, 6-week-old *N. benthamiana* leaves were infiltrated with combined *pAcANS::GUS/35S::AcMYB123/35S::AcbHLH42*. Three days after infiltration, the injected leaf tissues were collected and cut into 1-cm diameter discs.

The *N. benthamiana* leaf discs were histochemically stained with 5-bromo-4-chloro-3-indolyl β-D-glucuronide (X-Gluc) for 24 h at 37°C following the procedure described in Liu *et al.* (2012) then incubated in 70% ethanol to remove the chlorophyll before photographing. For measurements of the GUS activity, 4-MUG (Sigma-Aldrich, <http://www.sigmaaldrich.com/>) was added as a substrate for fluorometric assay as previously described (Jefferson, 1988), and the 4-MU produced in the GUS reaction was measured by a Thermo Scientific Microplate Reader (Thermo Scientific, <http://www.thermofisher.com/>). The total concentration of protein extracted from the leaf discs was measured using a Pierce™ BCA Protein Assay (Thermo Scientific) and diluted to a reaction concentration of 50 µg ml<sup>-1</sup>. Final GUS activity was calculated according to the standard curve of 4-MU (Sigma Aldrich) and expressed as nmol MU min<sup>-1</sup> µg<sup>-1</sup> protein. The GUS assays were repeated three times.

### Transient expression of *AcMYB123* and *AcbHLH42* in *N. tabacum*

*Agrobacterium tumefaciens* strain GV3101 containing the constructs 35S::*AcMYB123*, 35S::*AcbHLH42* or an equal mixture of 35S::*AcMYB123* and 35S::*AcbHLH42*, as well as an empty vector (pHB), were independently infiltrated into the 6-week-old *N. tabacum* leaves for transient transformation. *Nicotiana tabacum* transient expression assay was performed as previously described (Niu *et al.*, 2010b). Five days after infiltration, changes in leaf color, gene expression and anthocyanin content in the corresponding injection regions of the same injected leaves were recorded. The experiment was repeated three times.

### Subcellular localization

The coding regions of *AcMYB123* and *AcbHLH42* were amplified with the primers listed in Table S2 and then cloned into the vector of pART27-GFP, which contains green fluorescent protein (GFP) driven by the CaMV35S promoter (Zhang *et al.*, 2015), to generate constructs pART27-*AcMYB123*-GFP and pART27-*AcbHLH42*-GFP. These constructs were then introduced into *N. benthamiana* protoplasts by polyethylene glycol (PEG)-mediated transformation following the procedure described previously (Yoo *et al.*, 2007). The GFP transiently expressed in protoplasts was observed under a Leica TCS SP1 confocal microscope using three-channel measurement of emission, 435 nm [blue/4',6-diamidino-2-phenylindole (DAPI)], 522 nm (green/GFP) and 680 nm (red/chlorophyll).

### Bimolecular fluorescence complementation analysis

The coding region of *AcMYB123* was cloned into the pSPYNE vector containing the N-terminal 155 amino acids of yellow fluorescent protein (YFP) to generate pSPYNE-*AcMYB123*, whereas *AcbHLH42* was inserted into the pSPYCE vector containing the C-terminal 83 amino acids of YFP to generate pSPYCE-*AcbHLH42* (Walter *et al.*, 2004). The primers used in the relevant constructs are listed in Table S2. For the BiFC assay, *N. benthamiana* protoplasts were isolated and PEG-mediated transformation was conducted as previously described (Yoo *et al.*, 2007). After incubation for 16–20 h at 23°C, the protoplasts were detected by a confocal microscope (Leica TCS SPE, <https://www.leica-microsystems.com/>) using three-channel measurement of emission, 435 nm (blue/DAPI), 515 nm (green/YFP) and 680 nm (red/chlorophyll).

### Co-immunoprecipitation

Coding regions of *AcMYB123* and *AcbHLH42* were PCR-amplified (primers listed in Table S2) and cloned into pBTEX (Xiao *et al.*, 2007). The resulting CaMV35S promoter-driven constructs, pBTEX-*AcMYB123*-HA and pBTEX-*AcbHLH42*-FLAG, were introduced into *A. tumefaciens* GV3101. *Agrobacterium*-mediated transient expression was carried out as described previously (Xiao *et al.*, 2007; Miao *et al.*, 2016). Infected *N. benthamiana* leaf tissues were collected at 36 h after infiltration and ground to a fine powder with liquid nitrogen. The lysate was resuspended in 1.0 ml of protein extraction buffer [50 mM TRIS-HCl pH 7.5, 150 mM NaCl, 5 mM EDTA, 2 mM dithiothreitol (DTT), 10% glycerol, 1% polyvinylpyrrolidone, 1 mM phenylmethylsulfonyl fluoride (PMSF), 10  $\mu$ l plant protease inhibitor cocktail] and centrifuged at 12 000g for 20 min at 4°C. The supernatant was incubated with 15  $\mu$ L  $\alpha$ -HA affinity matrix (Roche Applied Sciences, <http://lifescience.roche.com/>) at 4°C for 2 h to capture the epitope-tagged protein. After washing four times with washing buffer (50 mM

TRIS-HCl, pH 7.5, 250 mM NaCl, 5 mM EDTA, 10% glycerol, 1 mM PMSF), the immunoprecipitated protein complex was separated by SDS-PAGE and then subjected to Western blotting analysis using the  $\alpha$ -HA or  $\alpha$ -FLAG antibody.

### RNA interference of *AcMYB123*, *AcbHLH42*, *AcF3GT1* and *AcANS* in Hongyang

Forward and reverse PCR-amplified cDNA fragments of *AcANS*, *AcF3GT1*, *AcMYB123* or *AcbHLH42* (primers for amplification are listed in Table S2) were inserted into the 2 $\times$  CaMV35S-driven vector pHB to produce RNAi constructs 35S::*AcMYB123*-RNAi, 35S::*AcbHLH42*-RNAi, 35S::*AcF3GT1*-RNAi and 35S::*AcANS*-RNAi. The RNAi constructs and the empty pHB vector were independently transformed into *A. tumefaciens* strain GV3101. *Agrobacterium tumefaciens* culture (0.4 ml, OD<sub>600</sub> = 0.8) containing individual RNAi constructs or the empty vector was injected into the Hongyang fruits at 70 DAA through the top or bottom of the fruits using a 1-ml sterile syringe. The fruits were harvested at 20–30 days after injection. The inner pericarp from the fruits was collected for RNA extraction and anthocyanin measurement. The experiment was carried out with at least three biological replicates.

### Co-overexpression of *AcMYB123* and *AcbHLH42* in *A. argute* and *A. thaliana*

The full coding region of *AcMYB123* or *AcbHLH42* was obtained through PCR amplification of cDNAs using primers listed in Table S2, and then inserted into the pHB vector to generate the 35S::*AcMYB123* and 35S::*AcbHLH42* constructs. The recombinant vectors were independently transformed into *A. tumefaciens* strain GV3101. *Agrobacterium tumefaciens* culture (0.2 ml, OD<sub>600</sub> = 0.8) containing 35S::*AcMYB123*/35S::*AcbHLH42* or empty pHB vector was injected into the fruits of kiwifruit cv. Baby Star (*A. argute*), which has green flesh, 100 DAA through the top or bottom of the fruits using a 1-ml sterile syringe. At the fifth day after injection, fruits were collected for RNA extraction and anthocyanin measurement. The experiment was carried out with at least three biological replicates.

To generate transgenic Arabidopsis plants, the recombinant vectors 35S::*AcMYB123* and 35S::*AcbHLH42* were independently transformed into wild-type *A. thaliana* (Columbia) using the GV3101-mediated floral dipping method (Clough and Bent, 1998). Homozygous transformed progenies overexpressing either *AcMYB123* or *AcbHLH42* were screened on 1/2 MS medium with 50  $\mu$ g ml<sup>-1</sup> Basta (Sigma, <http://www.sigmaaldrich.com/>). Transgenic lines simultaneously overexpressing both *AcMYB123* and *AcbHLH42* were obtained by cross-pollination. Wild-type and all transgenic lines with different genotypes were germinated on the 1/2 MS medium by aseptic operation. Changes in seedling color were recorded at 8 days and measurement of anthocyanin or semi-quantitative RT-PCR detection of the transgene expression was conducted as described above.

### Sequence analysis

The amino acid sequences of kiwifruit *AcMYB123*, *AcbHLH42* and their homologs from other plant species were collected from the Kiwifruit Information Resource (<http://bdg.hfut.edu.cn/kir/index.html>) and National Center for Biotechnology Information (<https://www.ncbi.nlm.nih.gov/>). Protein sequences of MYB and bHLH members were aligned using Clustal W (Chenna *et al.*, 2003). A phylogenetic tree was constructed using the MEGA 5.0 program (Tamura *et al.*, 2011) with the neighbor-joining (NJ) method (Saitou and Nei, 1987) and 1000 bootstrap replicates.

## Statistical analysis

All statistical analyses were carried out using SPSS Statistics v.17.0. Total anthocyanin content and relative expression data were analyzed by one-way ANOVA. Tukey media comparison analysis was performed. Results are represented as means  $\pm$  standard deviation (SD). Differences at  $P < 0.05$  were considered as significant.

## ACKNOWLEDGEMENTS

This work was supported by grants from the National Natural Science Foundation of China (31700266 and 31471157), the National Foundation for Germplasm Repository of Special Horticultural Crops in Central Mountain Areas of China (NJF2017-69), the National Science Fund for Distinguished Young Scholars (30825030), Key Project from the Government of Sichuan Province (2013NZ0014), Key Project from the Government of Anhui Province (2012AKKG0739; 1808085MC57) and the US National Science Foundation (IOS-1339287 and IOS-1539831).

## CONFLICT OF INTEREST

The authors declare no conflicts of interest.

## SUPPORTING INFORMATION

Additional Supporting Information may be found in the online version of this article.

**Figure S1.** Scatter plot of genome-wide mRNA expression between two replicates of inner or outer pericarp tissues at 90 days after anthesis in *Actinidia chinensis* cv. Hongyang.

**Figure S2.** Validation of upregulated genes in the inner pericarp of *Actinidia chinensis* cv. Hongyang that are potentially related to anthocyanin biosynthesis.

**Figure S3.** Phylogenetic analysis of AcMYB123 and its homologous proteins.

**Figure S4.** Amino acid sequence alignment of putative anthocyanin-related MYB transcription factors.

**Figure S5.** Phylogenetic analysis of AcbHLH42 and its homologous proteins.

**Figure S6.** Subcellular localization of AcMYB123 and AcbHLH42.

**Figure S7.** Interactions between AcMYB123 and AcMYBF110 or AcMYBF110 and AcbHLH42.

**Figure S8.** The HPLC chromatogram of anthocyanin composition in fruit of *Actinidia Chinensis* cv. Hongyang.

**Figure S9.** Structure of fruit tissues transiently expressing plasmid constructs of empty vector, 35S::AcMYB123-RNAi or 35S::AcbHLH42-RNAi in *Actinidia Chinensis* cv. Hongyang.

**Figure S10.** Quantitative RT-PCR detection of off-targets in the RNA interference suppression fruits.

**Figure S11.** Action of AcMYBF110 alone or combinatorial expression of AcMYBF110 and AcbHLH42 in determining anthocyanin production in transiently expressed *Nicotiana tabacum* leaves.

**Figure S12.** cis-regulatory elements detected in promoters of AcMYB123 and AcMYBF110.

**Figure S13.** Expression patterns of the previously characterized anthocyanin-related MYBs in *Actinidia chinensis* cv. Hongyang.

**Figure S14.** Enhanced expression of MYBs by co-expressing AcMYB123 and AcbHLH42 in *Actinidia arguta* cv. Baby star.

**Figure S15.** Transactivation of AcMYB123, AcMYBF110 and AcbHLH42 by GUS activity assays.

**Figure S16.** Expression pattern of AcDFR in *Actinidia chinensis* cv. Hongyang.

**Figure S17.** cis-regulatory elements in promoters of anthocyanin biosynthetic genes.

**Figure S18.** Proanthocyanidin accumulation and biosynthesis-related gene expression detected in *Actinidia chinensis* cv. Hongyang.

**Figure S19.** Expression pattern of Acc03242/Ach03g045741 in fruit of *Actinidia chinensis* cv. Hongyang.

**Figure S20.** Interactions between Acc03242/Ach03g045741 and either AcbHLH42 or AcMYB123.

**Table S1.** Differentially expressed genes between inner and outer pericarp in *A. chinensis* cv. Hongyang. DEGs between E19 E20 and E21 E22

**Table S2.** Primers used in this paper.

## REFERENCES

- Albert, N.W., Davies, K.M., Lewis, D.H., Zhang, H., Montefiori, M., Brendolise, C., Boase, M.R., Ngo, H., Jameson, P.E. and Schwinn, K.E. (2014) A conserved network of transcriptional activators and repressors regulates anthocyanin pigmentation in eudicots. *Plant Cell*, **26**, 962–980.
- An, X.H., Tian, Y., Chen, K.Q., Wang, X.F. and Hao, Y.J. (2012) The apple WD40 protein MdTTG1 interacts with bHLH but not MYB proteins to regulate anthocyanin accumulation. *J. Plant Physiol.* **169**, 710–717.
- Baudry, A., Heim, M.A., Dubreucq, B., Caboche, M., Weisshaar, B. and Lepiniec, L. (2004) TT2, TT8, and TTG1 synergistically specify the expression of BANYULS and proanthocyanidin biosynthesis in *Arabidopsis thaliana*. *Plant J.* **39**, 366–380.
- Baudry, A., Caboche, M. and Lepiniec, L. (2006) TT8 controls its own expression in a feedback regulation involving TTG1 and homologous MYB and bHLH factors, allowing a strong and cell-specific accumulation of flavonoids in *Arabidopsis thaliana*. *Plant J.* **46**, 768–779.
- Benjamini, Y. and Hochberg, Y. (1995) Controlling the false discovery rate: a practical and powerful approach to multiple testing. *J. R. Stat. Soc. B*, **57**, 289–300.
- Ben-Simhon, Z., Judeinstein, S., Nadler-Hassar, T., Trainin, T., Bar-Ya'akov, I., Borochoy-Neori, H. and Holland, D. (2011) A pomegranate (*Punica granatum* L.) WD40-repeat gene is a functional homologue of Arabidopsis TTG1 and is involved in the regulation of anthocyanin biosynthesis during pomegranate fruit development. *Planta*, **234**, 865–881.
- Bolger, A.M., Lohse, M. and Usadel, B. (2014) Trimmomatic: a flexible trimmer for Illumina sequence data. *Bioinformatics*, **30**, 2114–2120.
- Borevitz, J.O., Xia, Y., Blount, J., Dixon, R.A. and Lamb, C. (2000) Activation tagging identifies a conserved MYB regulator of phenylpropanoid biosynthesis. *Plant Cell*, **12**, 2383–2394.
- Boss, P.K., Davies, C. and Robinson, S.P. (1996) Analysis of the expression of anthocyanin pathway genes. *Plant Physiol.* **111**, 1059–1066.
- Carey, C.C., Strahle, J.T., Selinger, D.A. and Chandler, V.L. (2004) Mutations in the pale aleurone color1 regulatory gene of the Zea mays anthocyanin pathway have distinct phenotypes relative to the functionally similar TRANSPARENT TESTA GLABRA1 gene in *Arabidopsis thaliana*. *Plant Cell*, **16**, 450–464.
- Chandler, V.L. (1989) Two regulatory genes of the maize anthocyanin pathway are homologous: isolation of B utilizing R genomic sequences. *Plant Cell Online*, **1**, 1175–1183.
- Chen, P.Y., Wang, C.K., Soong, S.C. and To, K.Y. (2003) Complete sequence of the binary vector pBI121 and its application in cloning T-DNA insertion from transgenic plants. *Mol. Breed.* **11**, 287–293.
- Chenna, R., Sugawara, H., Koike, T., Lopez, R., Gibson, T.J., Higgins, D.G. and Thompson, J.D. (2003) Multiple sequence alignment with the Clustal series of programs. *Nucleic Acids Res.* **31**, 3497–3500.
- Clough, S.J. and Bent, A.F. (1998) Floral dip: a simplified method for Agrobacterium-mediated transformation of *Arabidopsis thaliana*. *Plant J.* **16**, 735–743.
- Comeskey, D.J., Montefiori, M., Edwards, P.J.B. and McGhie, T.K. (2009) Isolation and structural identification of the anthocyanin components of red kiwifruit. *J. Agric. Food Chem.* **57**, 2035–2039.
- Cone, K.C., Burr, F.A. and Burr, B. (1986) Molecular analysis of the maize anthocyanin regulatory locus C1. *Proc. Natl Acad. Sci. USA*, **83**, 9631–9635.
- Cutanda-Perez, M.C., Ageorges, A., Gomez, C., Vialet, S., Terrier, N., Romieu, C. and Torregrasa, L. (2009) Ectopic expression of VlmbyA1 in

- grapevine activates a narrow set of genes involved in anthocyanin synthesis and transport. *Plant Mol. Biol.*, **69**, 633–648.
- Dawes, H.M. and Keene, J.B.** (1999) Phenolic composition of kiwifruit juice. *J. Agric. Food Chem.* **47**, 2398–2403.
- Deluc, L., Bogs, J., Walker, A.R., Ferrier, T., Decendit, A., Merillon, J.-M., Robinson, S.P. and Barrieu, F.** (2008) The transcription factor VvMYB5b contributes to the regulation of anthocyanin and proanthocyanidin biosynthesis in developing grape berries. *Plant Physiol.* **147**, 2041–2053.
- Devic, M., Guilleminot, J., Debeaujon, I., Bechtold, N., Bensaude, E., Koornneef, M., Pelletier, G. and Delseny, M.** (1999) The BANYULS gene encodes a DFR-like protein and is a marker of early seed coat development. *Plant J.* **19**, 387–398.
- Dobin, A. and Gingeras, T.R.** (2016) Optimizing RNA-seq mapping with STAR. *Methods Mol. Biol.* 245–262.
- Du, H., Zhang, L., Liu, L., Tang, X.F., Yang, W.J., Wu, Y.M., Huang, Y.B. and Tang, Y.X.** (2009) Biochemical and molecular characterization of plant MYB transcription factor family. *Biochemistry*, **74**, 1–11.
- Dubos, C., Gourrierc, J.Le, Baudry, A. et al.** (2008) MYBL2 is a new regulator of flavonoid biosynthesis in *Arabidopsis thaliana*. *Plant J.* **55**, 940–953.
- Feller, A., MacHemer, K., Braun, E.L. and Grotewold, E.** (2011) Evolutionary and comparative analysis of MYB and bHLH plant transcription factors. *Plant J.* **66**, 94–116.
- Feng, S., Wang, Y., Yang, S., Xu, Y. and Chen, X.** (2010) Anthocyanin biosynthesis in pears is regulated by a R2R3-MYB transcription factor PyMYB10. *Planta*, **232**, 245–255.
- Fraser, L.G., Seal, A.G., Montefiori, M. et al.** (2013) An R2R3 MYB transcription factor determines red petal colour in an *Actinidia* (kiwifruit) hybrid population. *BMC Genom.*, **14**, 28.
- Gonzalez, A., Zhao, M., Leavitt, J.M. and Lloyd, A.M.** (2008) Regulation of the anthocyanin biosynthetic pathway by the TTG1/bHLH/Myb transcriptional complex in *Arabidopsis* seedlings. *Plant J.* **53**, 814–827.
- Griesser, M., Hoffmann, T., Bellido, M.L., Rosati, C., Fink, B., Kurtzer, R., Aharoni, A., Munoz-Blanco, J. and Schwab, W.** (2008) Redirection of flavonoid biosynthesis through the down-regulation of an anthocyanidin glucosyltransferase in ripening strawberry fruit. *Plant Physiol.* **146**, 1528–1539.
- Grotewold, E.** (2006) The genetics and biochemistry of floral pigments. *Annu. Rev. Plant Biol.* **57**, 761–780.
- Grotewold, E., Sainz, M.B., Tagliani, L., Hernandez, J.M., Bowen, B. and Chandler, V.L.** (2000) Identification of the residues in the Myb domain of maize C1 that specify the interaction with the bHLH cofactor R. *Proc. Natl Acad. Sci. USA*, **97**, 13579–13584.
- Hichri, I., Heppel, S.C., Pillet, J., Léon, C., Czemplak, S., Delrot, S., Lauvergeat, V. and Bogs, J.** (2010) The basic helix-loop-helix transcription factor MYC1 is involved in the regulation of the flavonoid biosynthesis pathway in grapevine. *Mol. Plant*, **3**, 509–523.
- Hichri, I., Barrieu, F., Bogs, J., Kappel, C., Delrot, S. and Lauvergeat, V.** (2011) Recent advances in the transcriptional regulation of the flavonoid biosynthetic pathway. *J. Exp. Bot.* **62**, 2465–2483.
- Higo, K., Ugawa, Y., Iwamoto, M. and Korenaga, T.** (1999) Plant cis-acting regulatory DNA elements (PLACE) database: 1999. *Nucleic Acids Res.* **27**, 297–300.
- Honda, C., Kotoda, N., Wada, M., Kondo, S., Kobayashi, S., Soejima, J., Zhang, Z., Tsuda, T. and Moriguchi, T.** (2002) Anthocyanin biosynthetic genes are coordinately expressed during red coloration in apple skin. *Plant Physiol. Biochem.* **40**, 955–962.
- Huang, S., Ding, J., Deng, D. et al.** (2013) Draft genome of the kiwifruit *Actinidia chinensis*. *Nat. Commun.* **4**, 2640.
- Huguene, P., Provenzano, S., Verries, C. et al.** (2009) A novel cation-dependent O-methyltransferase involved in anthocyanin methylation in grapevine. *Plant Physiol.* **150**, 2057–2070.
- Jefferson, R.** (1988) Plant reporter genes: the GUS gene fusion system. *Genet. Eng. Princ. Methods*, 247–263.
- Jin, H. and Martin, C.** (1999) Multifunctionality and diversity within the plant MYB-gene family. *Plant Mol. Biol.* **41**, 577–585.
- Koes, R., Verweij, W. and Quattrocchio, F.** (2005) Flavonoids: a colorful model for the regulation and evolution of biochemical pathways. *Trends Plant Sci.* **10**, 236–242.
- Lea, U.S., Slimestad, R. and Smedvig, P.** (2007) Nitrogen de W ciency enhances expression of speci W c MYB and bHLH transcription factors and accumulation of end products in the X avonoid pathway. *Planta*, **225**, 1245–1253.
- Li, M., Ma, F., Liang, D., Li, J. and Wang, Y.** (2010) Ascorbate biosynthesis during early fruit development is the main reason for its accumulation in kiwi. *PLoS One*, **5**.
- Li, Y., Van den Ende, W. and Rolland, F.** (2014) Sucrose induction of anthocyanin biosynthesis is mediated by DELLA. *Mol. Plant*, **7**, 570–572.
- Li, B., Xia, Y., Wang, Y., Qin, G. and Tian, S.** (2017a) Characterization of genes encoding key enzymes involved in anthocyanin metabolism of kiwifruit during storage period. *Front. Plant Sci.* **8**, 1–8.
- Li, W., Ding, Z., Ruan, M., Yu, X., Peng, M. and Liu, Y.** (2017b) Kiwifruit R2R3-MYB transcription factors and contribution of the novel AcMYB75 to red kiwifruit anthocyanin biosynthesis. *Sci. Rep.* **7**, 16861.
- Lillo, C., Lea, U.S. and Ruoff, P.** (2008) Nutrient depletion as a key factor for manipulating gene expression and product formation in different branches of the flavonoid pathway. *Plant, Cell Environ.* **31**, 587–601.
- Liu, J., Li, H., Miao, M., Tang, X., Giovannoni, J., Xiao, F. and Liu, Y.** (2012) The tomato UV-damaged DNA-binding protein-1 (DDB1) is implicated in pathogenesis-related (PR) gene expression and resistance to *Agrobacterium tumefaciens*. *Mol. Plant Pathol.* **13**, 123–134.
- Liu, X., Feng, C., Zhang, M., Yin, X., Xu, C. and Chen, K.** (2013) The MrWD40-1 gene of Chinese bayberry (*Myrica rubra*) interacts with MYB and bHLH to enhance anthocyanin accumulation. *Plant Mol. Biol. Rep.* **31**, 1474–1484.
- Liu, Y., Zhou, B., Qi, Y., Chen, X., Liu, C., Liu, Z. and Ren, X.** (2017) Expression differences of pigment structural genes and transcription factors explain flesh coloration in three contrasting kiwifruit cultivars. *Front. Plant Sci.* **8**, 1–15.
- Livak, K.J. and Schmittgen, T.D.** (2001) Analysis of relative gene expression data using real-time quantitative PCR and the 2(-Delta Delta C(T)) Method. *Methods*, **25**, 402–408.
- Ludwig, S.R., Habera, L.F., Dellaporta, S.L. and Wessler, S.R.** (1989) Lc, a member of the maize R gene family responsible for tissue-specific anthocyanin production, encodes a protein similar to transcriptional activators and contains the myc-homology region. *Proc. Natl Acad. Sci. USA*, **86**, 7092–7096.
- Man, Y.P., Wang, Y.C., Li, Z.Z. et al.** (2015) High-temperature inhibition of biosynthesis and transportation of anthocyanins results in the poor red coloration in red-fleshed *Actinidia chinensis*. *Physiol. Plant.*, **153**, 565–583.
- Matsui, K., Umemura, Y. and Ohme-Takagi, M.** (2008) AtMYBL2, a protein with a single MYB domain, acts as a negative regulator of anthocyanin biosynthesis in *Arabidopsis*. *Plant J.* **55**, 954–967.
- Matus, J.T., Poupin, M.J., Cañón, P., Bordeu, E., Alcalde, J.A. and Arce-Johnson, P.** (2010) Isolation of WDR and bHLH genes related to flavonoid synthesis in grapevine (*Vitis vinifera* L.). *Plant Mol. Biol.* **72**, 607–620.
- Mehrtens, F.** (2005) The arabidopsis transcription factor MYB12 is a flavonol-specific regulator of phenylpropanoid biosynthesis. *Plant Physiol.* **138**, 1083–1096.
- Miao, M., Niu, X., Kud, J., Du, X., Avila, J., Devarenne, T.P., Kuhl, J.C., Liu, Y. and Xiao, F.** (2016) The ubiquitin ligase SEVEN IN ABSENTIA (SINA) ubiquitinates a defense-related NAC transcription factor and is involved in defense signaling. *New Phytol.* **211**, 138–148.
- Montefiori, M., McGhie, T.K., Costa, G. and Ferguson, A.R.** (2005) Pigments in the fruit of red-fleshed kiwifruit (*Actinidia chinensis* and *Actinidia deliciosa*). *J. Agric. Food Chem.* **53**, 9526–9530.
- Montefiori, M., Comeskey, D.J., Wohlers, M. and McGhie, T.K.** (2009) Characterization and quantification of anthocyanins in red kiwifruit (*Actinidia* spp.). *J. Agric. Food Chem.* **57**, 6856–6861.
- Montefiori, M., Easley, R.V., Stevenson, D., Cooney, J., Datson, P.M., Saiz, A., Atkinson, R.G., Hellens, R.P. and Allan, A.C.** (2011) Identification and characterisation of F3GT1 and F3GGT1, two glycosyltransferases responsible for anthocyanin biosynthesis in red-fleshed kiwifruit (*Actinidia chinensis*). *Plant J.* **65**, 106–118.
- Montefiori, M., Brendolise, C., Dare, A.P., Kui, L.W., Davies, K.M., Hellens, R.P. and Allan, A.C.** (2015) In the Solanaceae, a hierarchy of bHLHs confer distinct target specificity to the anthocyanin regulatory complex. *J. Exp. Bot.* **66**, 1427–1436.
- Nakatsuka, T., Saito, M., Yamada, E., Fujita, K., Kakizaki, Y. and Nishihara, M.** (2012) Isolation and characterization of GtMYBP3 and GtMYBP4, orthologues of R2R3-MYB transcription factors that regulate early flavonoid biosynthesis, in gentian flowers. *J. Exp. Bot.* **63**, 6505–6517.

- Nesi, N., Debeaujon, I., Jond, C., Pelletier, G., Caboche, M. and Lepiniec, L. (2000) The TT8 gene encodes a basic helix-loop-helix domain protein required for expression of DFR and BAN genes in *Arabidopsis siliques*. *Plant Cell* **12**, 1863–1878.
- Nesi, N., Jond, C., Debeaujon, I., Caboche, M. and Lepiniec, L. (2001) The Arabidopsis TT2 gene encodes an R2R3 MYB domain protein that acts as a key determinant for proanthocyanidin accumulation in developing seed. *Plant Cell* **13**, 2099–2114.
- Niu, X.S., Xu, C.J., Zhang, W.S., Zhang, B., Li, X., Lin-Wang, K., Ferguson, I.B., Allan, A.C. and Chen, K.S. (2010a) Coordinated regulation of anthocyanin biosynthesis in Chinese bayberry (*Myrica rubra*) fruit by a R2R3 MYB transcription factor. *Planta* **231**, 887–899.
- Niu, X., Luo, D., Gao, S. et al. (2010b) A conserved unusual posttranscriptional processing mediated by short, direct repeated (SDR) sequences in plants. *J. Genet. Genomics*, **37**, 85–99.
- Patra, B., Schluttenhofer, C., Wu, Y., Pattanaik, S. and Yuan, L. (2013) Transcriptional regulation of secondary metabolite biosynthesis in plants. *Biochim. Biophys. Acta - Gene Regul. Mech.* **1829**, 1236–1247.
- Paz-Ares, J., Ghosal, D., Wienand, U., Peterson, P.A. and Saedler, H. (1987) The regulatory c1 locus of *Zea mays* encodes a protein with homology to myb proto-oncogene products and with structural similarities to transcriptional activators. *EMBO J.* **6**, 3553–3558.
- Pilkington, S.M., Crowhurst, R., Hilario, E. et al. (2018) A manually annotated *Actinidia chinensis* var. *chinensis* (kiwifruit) genome highlights the challenges associated with draft genomes and gene prediction in plants. *BMC Genom.*, **19**, 257.
- Quattrocchio, F., Wing, J.F., Va, K., Mol, J.N. and Koes, R. (1998) Analysis of bHLH and MYB domain proteins: species-specific regulatory differences are caused by divergent evolution of target anthocyanin genes. *Plant J.* **13**, 475–488.
- Saitou, N. and Nei, M. (1987) The neighbor-joining method: a new method for reconstructing phylogenetic trees. *Mol. Biol. Evol.* **4**, 406–425.
- Schaart, J.G., Dubos, C., Romero De La Fuente, I. et al. (2013) Identification and characterization of MYB-bHLH-WD40 regulatory complexes controlling proanthocyanidin biosynthesis in strawberry (*Fragaria × ananassa*) fruits. *New Phytol.* **197**, 454–467.
- Schulze, S.K., Kanwar, R., Gözlenleuchter, M., Therneau, T.M. and Beutler, A.S. (2012) SERE: single-parameter quality control and sample comparison for RNA-Seq. *BMC, Genomics*, **13**.
- Shen, X., Zhao, K., Liu, L. et al. (2014) A role for PacMYBA in ABA-regulated anthocyanin biosynthesis in red-colored sweet cherry cv. Hong Deng (*Prunus avium* L.). *Plant Cell Physiol.*, **55**, 862–880.
- Stracke, R., Ishihara, H., Huep, G., Barsch, A., Mehrrens, F., Niehaus, K. and Weisshaar, B. (2007) Differential regulation of closely related R2R3-MYB transcription factors controls flavonol accumulation in different parts of the Arabidopsis thaliana seedling. *Plant J.*, **50**, 660–677.
- Takos, A.M., Jaffe, F.W., Jacob, S.R., Bogs, J., Robinson, S.P. and Walker, A.R. (2006) Light-induced expression of a MYB gene regulates anthocyanin biosynthesis in red apples. *Plant Physiol.* **142**, 1216–1232.
- Tamura, K., Peterson, D., Peterson, N., Stecher, G., Nei, M. and Kumar, S. (2011) MEGA5: molecular evolutionary genetics analysis using maximum likelihood, evolutionary distance, and maximum parsimony methods. *Mol. Biol. Evol.* **28**, 2731–2739.
- Tang, W., Zheng, Y., Dong, J. et al. (2016) Comprehensive transcriptome profiling reveals long noncoding RNA expression and alternative splicing regulation during fruit development and ripening in kiwifruit (*Actinidia chinensis*). *Front. Plant Sci.* **7**, 1–15.
- Tohge, T., Nishiyama, Y., Hirai, M.Y. et al. (2005) Functional genomics by integrated analysis of metabolome and transcriptome of Arabidopsis plants over-expressing an MYB transcription factor. *Plant J.* **42**, 218–235.
- Trapnell, C., Williams, B.A., Pertea, G., Mortazavi, A., Kwan, G., Baren, M.J., Van, Salzberg, S.L., Wold, B.J. and Pachter, L. (2010) Transcript assembly and quantification by RNA-Seq reveals unannotated transcripts and isoform switching during cell differentiation. *Nat. Biotechnol.* **28**, 511–515.
- Uematsu, C., Katayama, H., Makino, I., Inagaki, A., Arakawa, O. and Martin, C. (2014) Peace, a MYB-like transcription factor, regulates petal pigmentation in flowering peach “Genpei” bearing variegated and fully pigmented flowers. *J. Exp. Bot.* **65**, 1081–1094.
- Vetten, N.De, Quattrocchio, F., Mol, J. and Koes, R. (1997) The an11 locus controlling flower pigmentation in petunia encodes a novel WD-repeat protein conserved in yeast, plants, and animals. *Genes Dev.* **11**, 1422–1434.
- Walker, A.R., Davison, P.A., Bolognesi-Winfield, A.C., James, C.M., Srinivasan, N., Blundell, T.L., Esch, J.J., Marks, M.D. and Gray, J.C. (1999) The TRANSPARENT TESTA GLABRA1 locus, which regulates trichome differentiation and anthocyanin biosynthesis in Arabidopsis, encodes a WD40 repeat protein. *Plant Cell*, **11**, 1337–1349.
- Walker, A.R., Lee, E., Bogs, J., McDavid, D.A.J., Thomas, M.R. and Robinson, S.P. (2007) White grapes arose through the mutation of two similar and adjacent regulatory genes. *Plant J.* **49**, 772–785.
- Walter, M., Chaban, C., Schütze, K. et al. (2004) Visualization of protein interactions in living plant cells using bimolecular fluorescence complementation. *Plant J.* **40**, 428–438.
- Wang, N., Qu, C., Jiang, S. et al. (2018) The proanthocyanidin-specific transcription factor MdMYBPA1 initiates anthocyanin synthesis under low-temperature conditions in red-fleshed apples. *Plant J.* **96**, 39–55.
- Winkel-Shirley, B. (2001) Flavonoid biosynthesis: a colorful model for genetics, biochemistry, cell biology, and biotechnology. *Plant Physiol.* **126**, 485–493.
- Wu, R., Wang, T., McGie, T., Voogd, C., Allan, A.C., Hellens, R.P. and Varkonyi-Gasic, E. (2014) Overexpression of the kiwifruit SVP3 gene affects reproductive development and suppresses anthocyanin biosynthesis in petals, but has no effect on vegetative growth, dormancy, or flowering time. *J. Exp. Bot.* **65**, 4985–4995.
- Xiao, F., He, P., Abramovitch, R.B., Dawson, J.E., Nicholson, L.K., Sheen, J. and Martin, G.B. (2007) The N-terminal region of Pseudomonas type III effector AvrPtoB elicits Pto-dependent immunity and has two distinct virulence determinants. *Plant J.* **52**, 595–614.
- Xie, D.Y., Sharma, S.B., Paiva, N.L., Ferreira, D. and Dixon, R.A. (2003) Role of anthocyanidin reductase, encoded by BANYULS in plant flavonoid biosynthesis. *Science* **299**, 396–399.
- Xie, X., Bin, Li, S., Zhang, R.F. et al. (2012) The bHLH transcription factor MdbHLH3 promotes anthocyanin accumulation and fruit colouration in response to low temperature in apples. *Plant, Cell Environ.* **35**, 1884–1897.
- Xie, Y., Tan, H., Ma, Z. and Huang, J. (2016) DELLA proteins promote anthocyanin biosynthesis via sequestering MYBL2 and JAZ suppressors of the MYB/bHLH/WDR40 complex in *Arabidopsis thaliana*. *Mol. Plant*, **9**, 711–721.
- Xu, W., Dubos, C. and Lepiniec, L. (2015) Transcriptional control of flavonoid biosynthesis by MYB-bHLH-WDR complexes. *Trends Plant Sci.* **20**, 176–185.
- Yang, Y., Li, R. and Qi, M. (2000) *In vivo* analysis of plant promoters and transcription factors by agroinfiltration of tobacco leaves. *Plant J.* **22**, 543–551.
- Yao, G., Ming, M., Allan, A.C. et al. (2017) Map-based cloning of the pear gene MYB114 identifies an interaction with other transcription factors to coordinately regulate fruit anthocyanin biosynthesis. *Plant J.* **92**, 437–451.
- Yoo, S.D., Cho, Y.H. and Sheen, J. (2007) Arabidopsis mesophyll protoplasts: a versatile cell system for transient gene expression analysis. *Nat. Protoc.* **2**, 1565–1572.
- Yu, H., Yin, J., Li, H., Yang, S. and Shen, Z. (2000) Construction and selection of the novel recombinant *Escherichia coli* strain for poly( $\beta$ -hydroxybutyrate) production. *J. Biosci. Bioeng.* **89**, 307–311.
- Yue, J., Liu, J., Ban, R., Tang, W., Deng, L., Fei, Z. and Liu, Y. (2015) Kiwifruit Information Resource (KIR): a comparative platform for kiwifruit genomics. *Database*, **2015**, bav113.
- Zhang, J., Tang, W., Huang, Y., Niu, X., Zhao, Y., Han, Y. and Liu, Y. (2015) Down-regulation of a LBD-like gene, OsIG1, leads to occurrence of unusual double ovules and developmental abnormalities of various floral organs and megagametophyte in rice. *J. Exp. Bot.* **66**, 99–112.
- Zimmermann, I.M., Heim, M.A., Weisshaar, B. and Uhrig, J.F. (2004) Comprehensive identification of *Arabidopsis thaliana* MYB transcription factors interacting with R/B-like BHLH proteins. *Plant J.* **40**, 22–34.